Mechanistic Study of Pyrazole Synthesis via Oxidation-Induced N-N Coupling of Diazatitanacycles

Yukun Cheng, Daniel N. Huh, and Ian A. Tonks*

Contributed from the Department of Chemistry, University of Minnesota – Twin Cities, 207 Pleasant St SE, Minneapolis MN 55455. Email: itonks@umn.edu

Supporting Information

NMR Characterization of 3

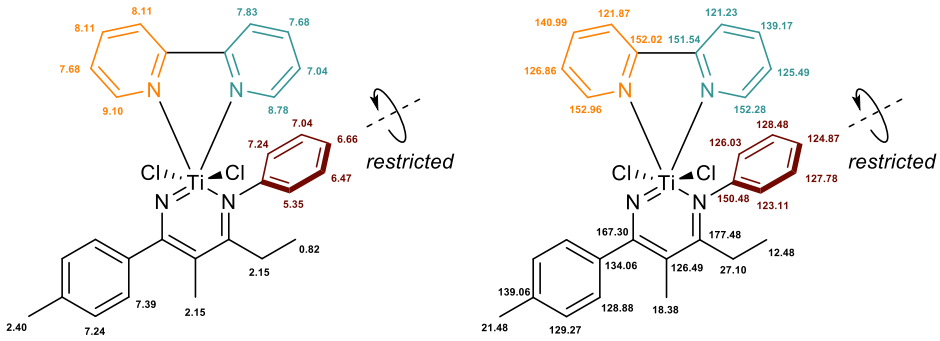

Figure S1. ^{1}H (left) and ^{13}C (right) signal assignments of **3**. Colors are labelled for clarity purpose to indicate the ring that the chemical shifts correspond to.

We sought evidence of the restricted rotation of *N*-phenyl on **3** from NOESY NMR spectrometry. As we expected, a through-space interaction between α-H of bpy and 2-H of *N*-phenyl was observed in the NOESY spectrum of **3**. In addition, the EXSY signals of the *N*-phenyl on its 2-H vs. 6-H and 3-H vs. 5-H indicate that these hydrogens are in exchange of one another. Together with the distinguishable chemical shift differences of the aforementioned hydrogens, these results provide strong evidence on the restricted rotation of *N*-phenyl.

To our surprise, EXSY signals were also found between the two pyridines of the bpy ligand on the NOESY spectrum of **3**, indicating that the bpy can undergo self-exchange between the two pyridines. This shows that bpy is a hemilabile ligand on **3**. On the other hand, the differences in ^{1}H and ^{13}C chemical shifts clearly indicates that the two pyridines are chemically inequivalent due to trans effect, which requires a strong coordination to Ti. It can be deduced that the bpy ligand on **3** is largely intact on Ti with a weak self-exchange at room temperature, while under elevated temperature the hemilability could be enhanced and eventually lead to the dissociation of the bpy ligand.

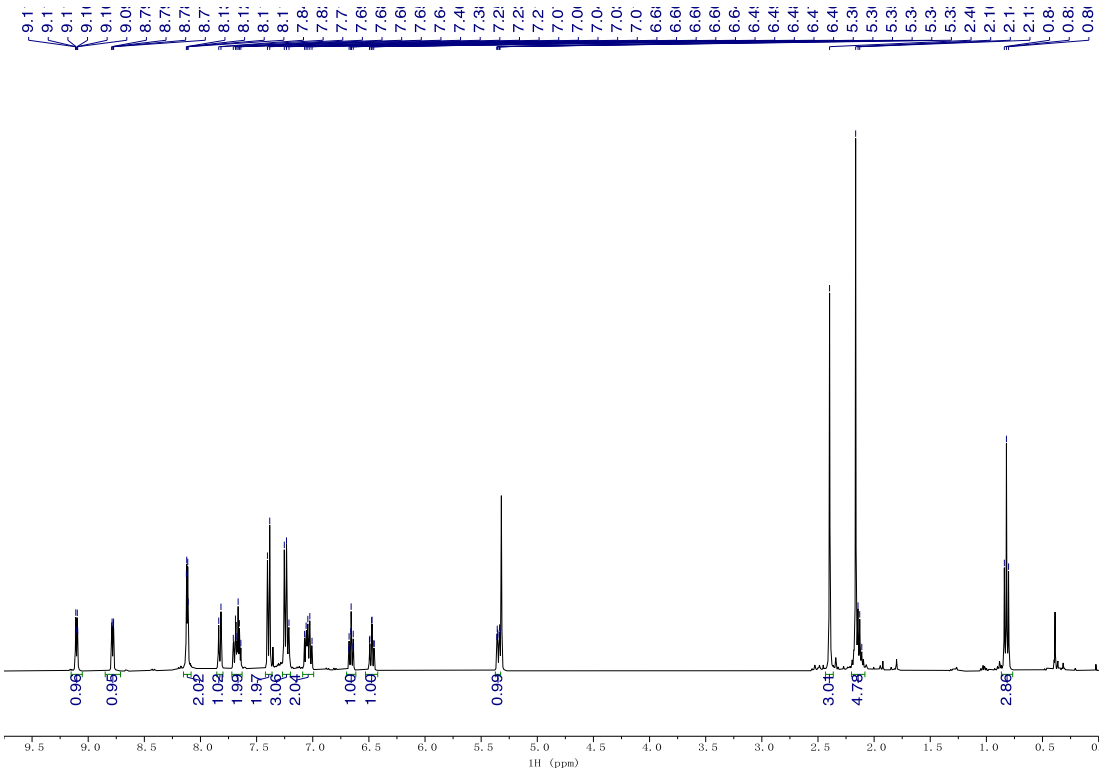

Figure S2. ^{1}H NMR spectrum of **3** (CD_2Cl_2, 400 MHz).

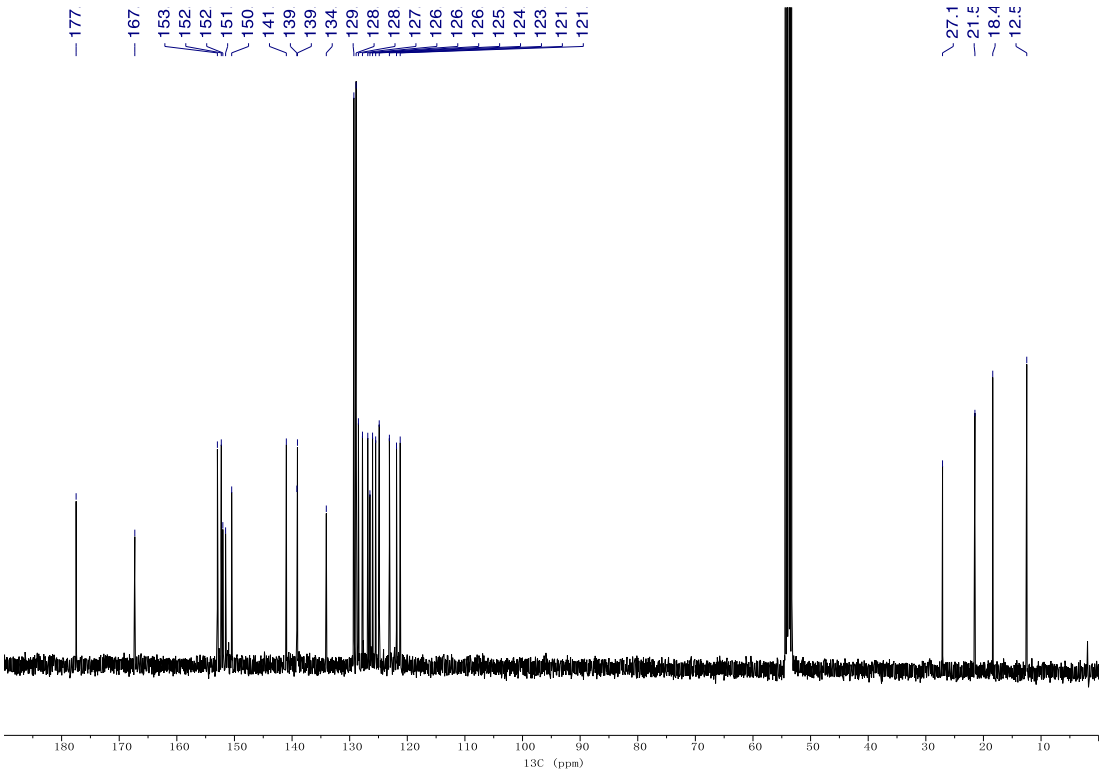

Figure S3. $^{13}C\{^{1}H\}$ NMR spectrum of **3** (CD_2Cl_2, 101 MHz).

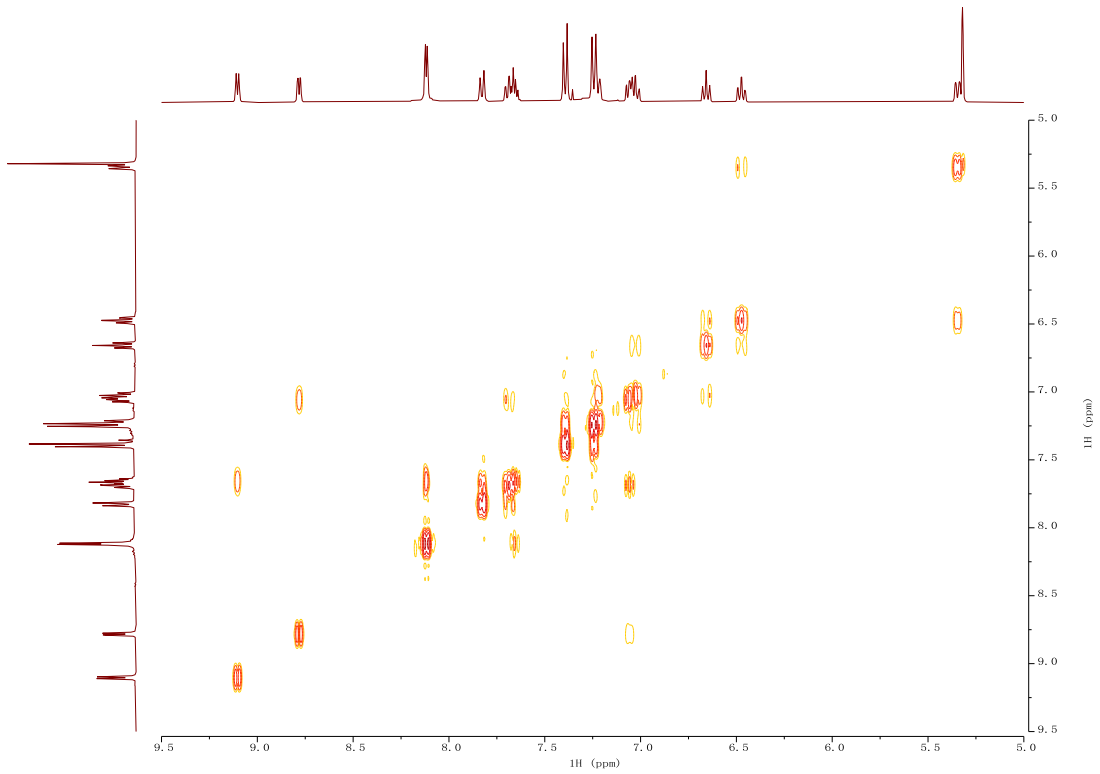

Figure S4. ^{1}H COSY NMR spectrum of **3** in CD_2Cl_2.

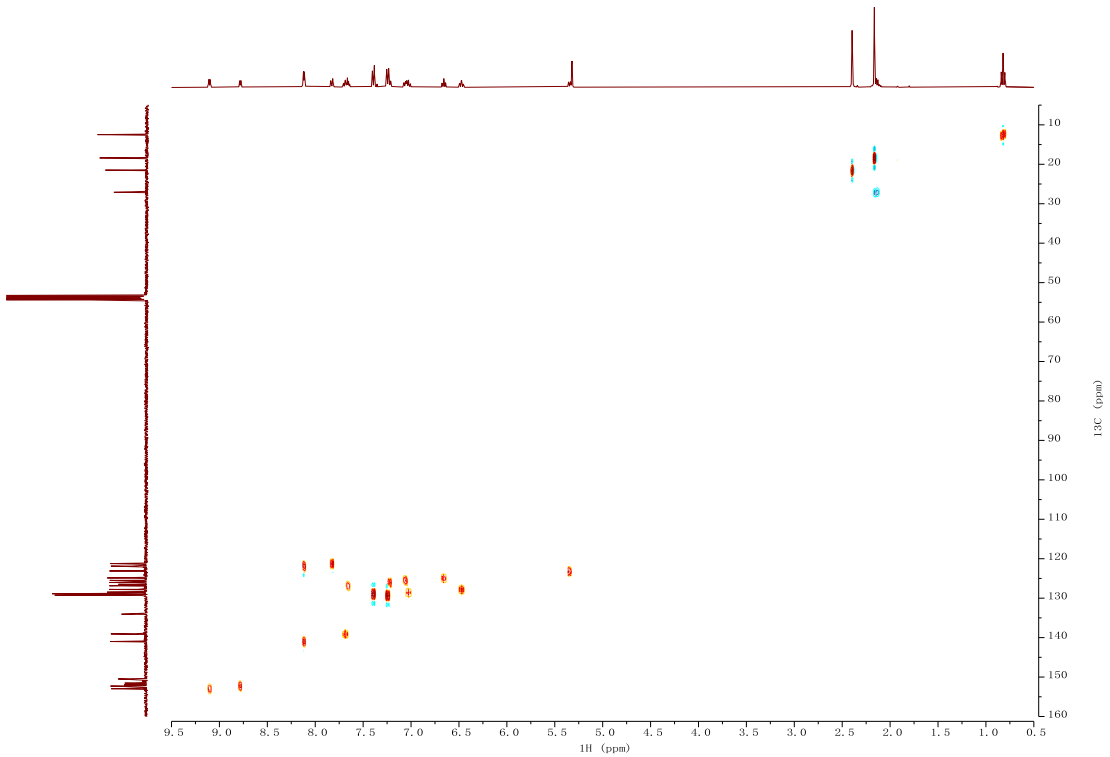

Figure S5. ^{1}H-^{13}C HSQC NMR spectrum of **3** in CD_2Cl_2.

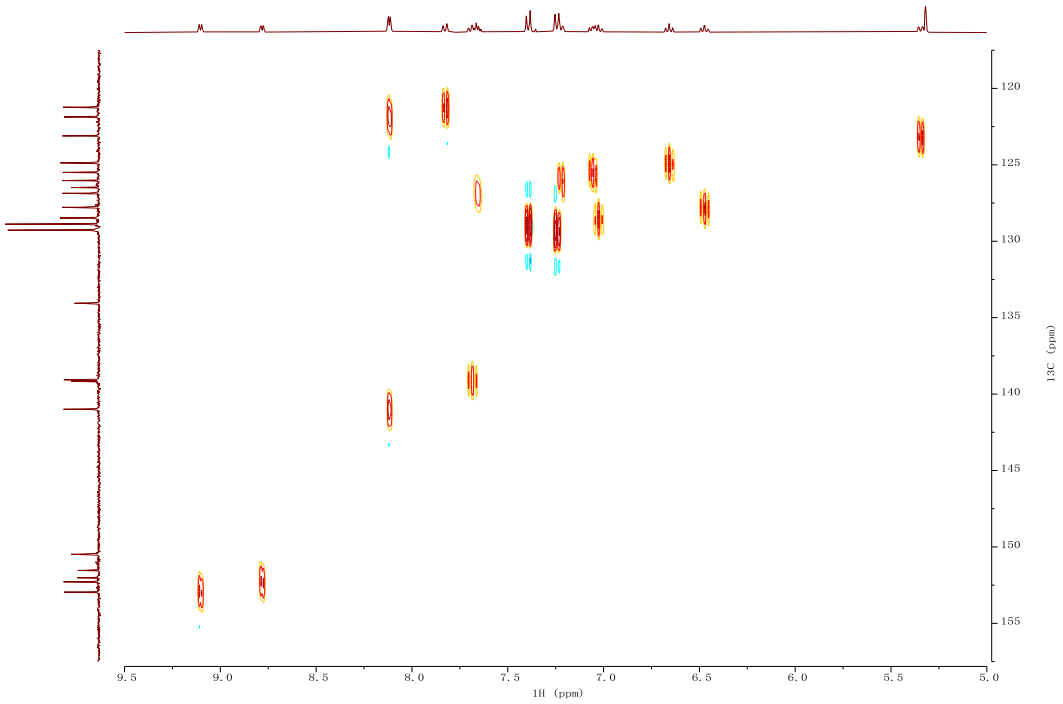

Figure S6. Aromatic region of ^{1}H-^{13}C HSQC NMR spectrum of **3** in CD_2Cl_2.

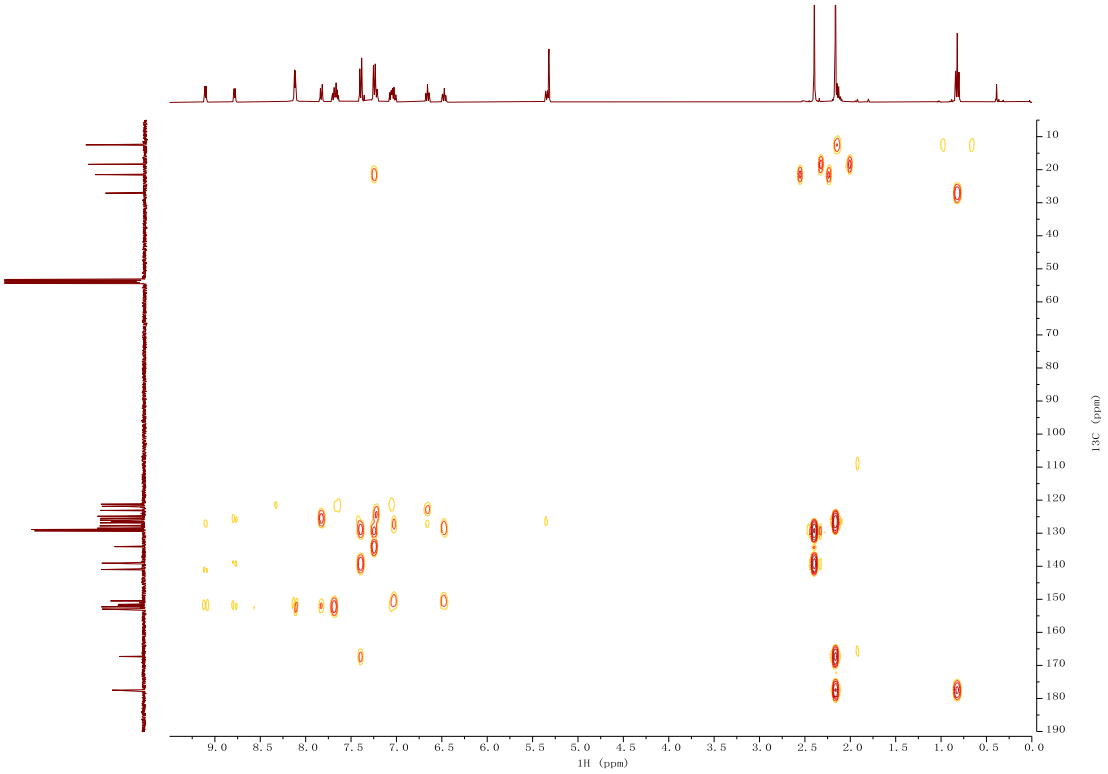

Figure S7. ^{1}H-^{13}C HMBC NMR spectrum of **3** in CD_2Cl_2.

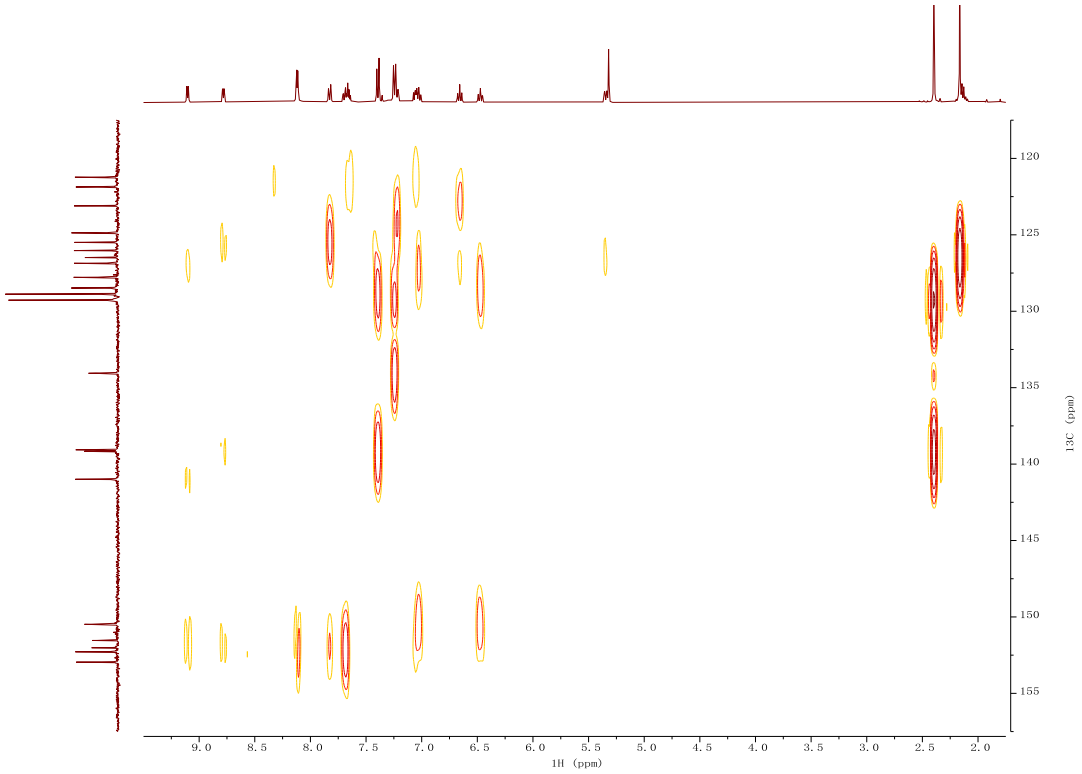

Figure S8. ^{13}C downfield region of ^{1}H-^{13}C HMBC NMR spectrum of **3** in CD_2Cl_2.

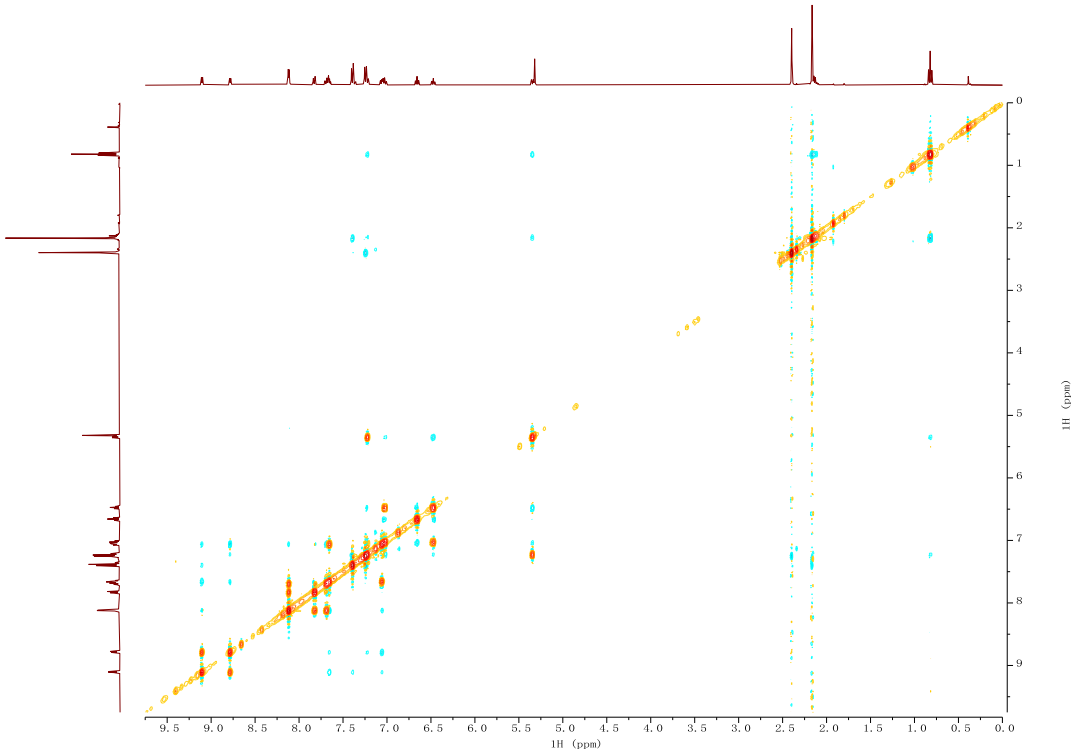

Figure S9. NOESY NMR spectrum of **3** in CD_2Cl_2 (full spectrum).

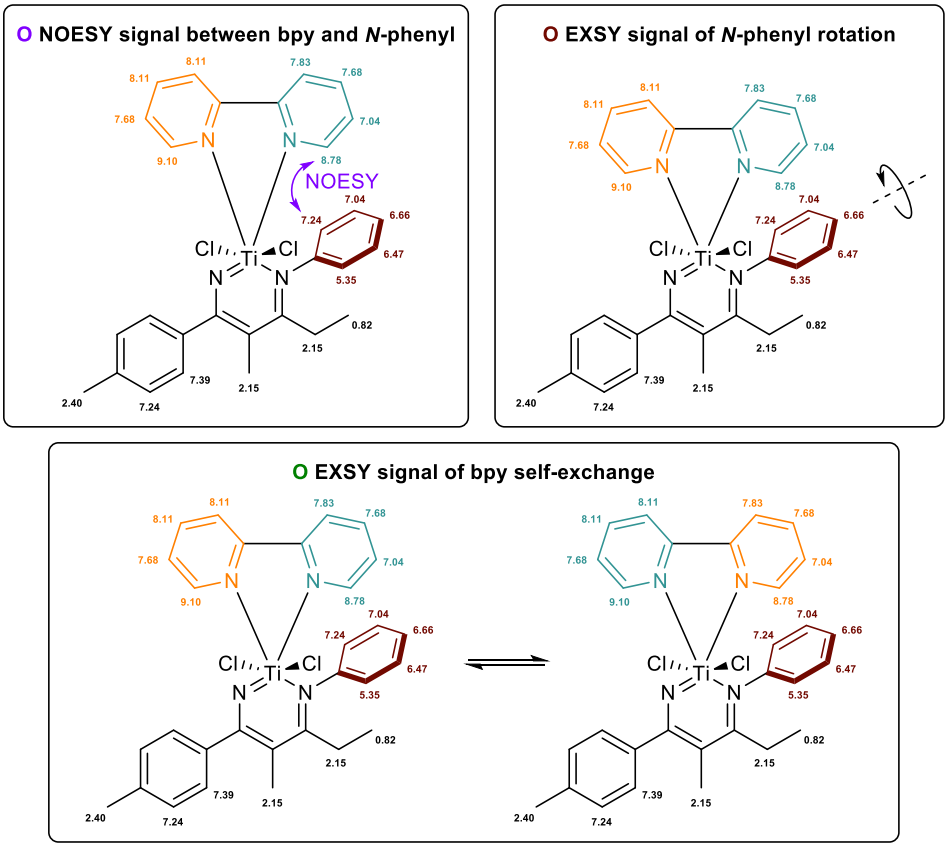
O NOESY signal between bpy and N-phenyl
NOESY
O EXSY signal of N-phenyl rotation
O EXSY signal of bpy self-exchange

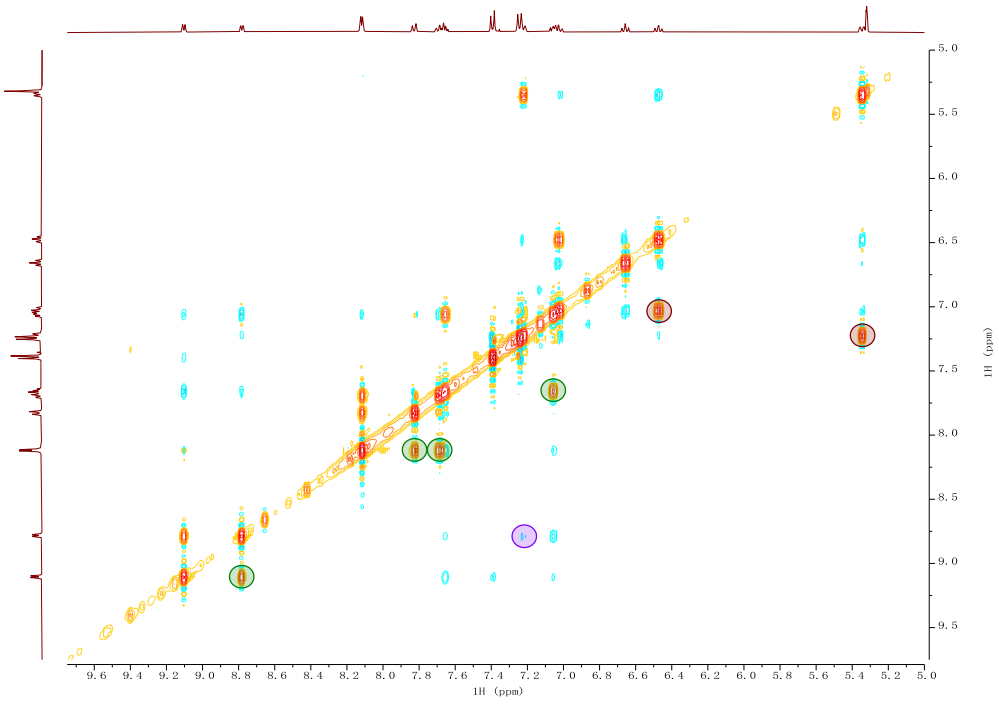
1H (ppm)
1H (ppm)

Figure S10. Aromatic region of NOESY NMR spectrum of **3** in CD_2Cl_2. Anti-phase NOESY and in-phase EXSY signal are labeled in corresponding colored circles denoting the modes of interaction. Signals on only one side of the diagonal are labeled for clarity purpose.

NMR Characterization of 1-dimer

Limited by the sample concentration, ^{13}C NMR signal of quaternary carbons were assigned with the assistance of ^{1}H-^{13}C HSQC and HMBC spectra.

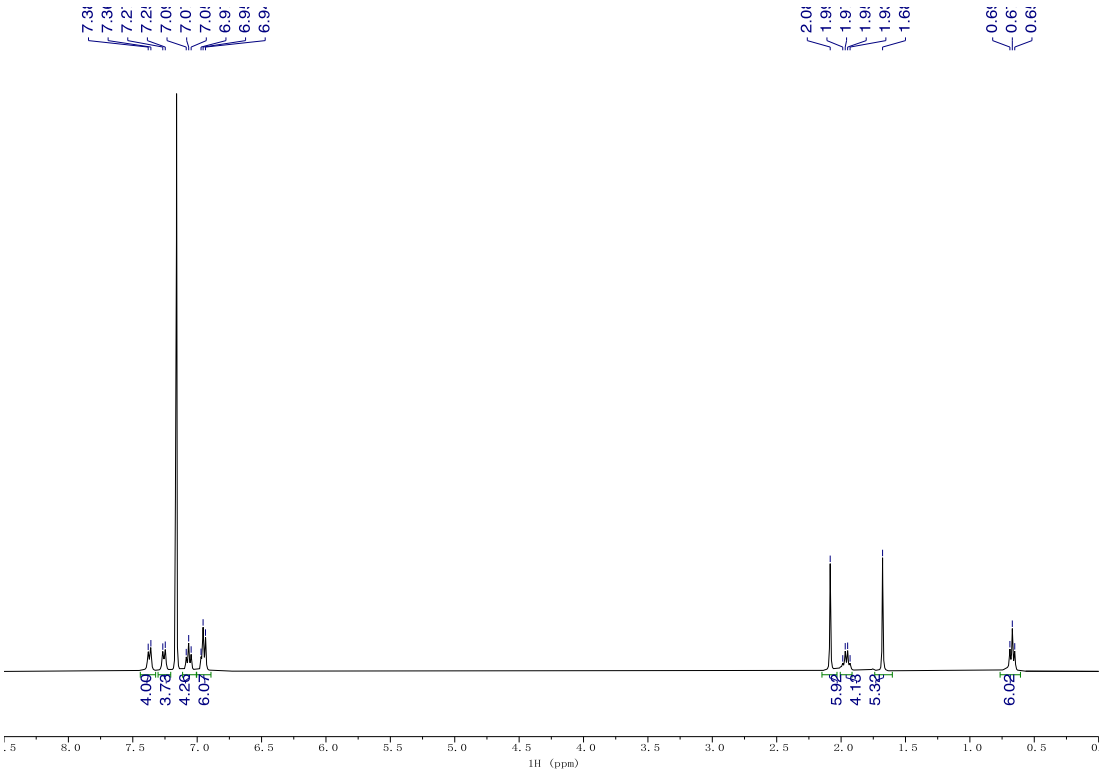

Figure S11. ^{1}H NMR spectrum of **1-dimer** (C_6D_6, 400 MHz) in the C_6D_6 solution of the mixture.

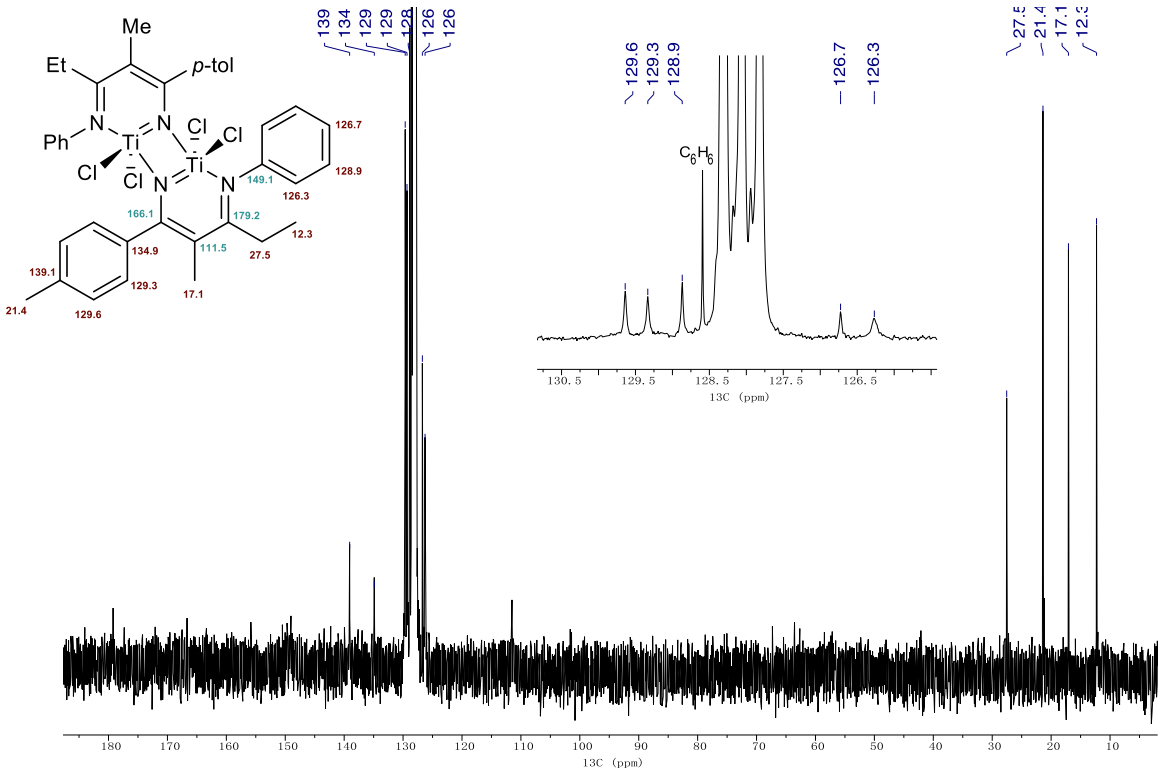

Figure S12. $^{13}C\{^{1}H\}$ NMR spectrum of **1-dimer** (C_6D_6, 125 MHz) in the C_6D_6 solution of the mixture and signal assignments. Chemical shifts in maroon were observed in $^{13}C\{^{1}H\}$ NMR spectrum. Chemical shifts in teal were determined *via* ^{1}H-^{13}C HMBC spectrum.

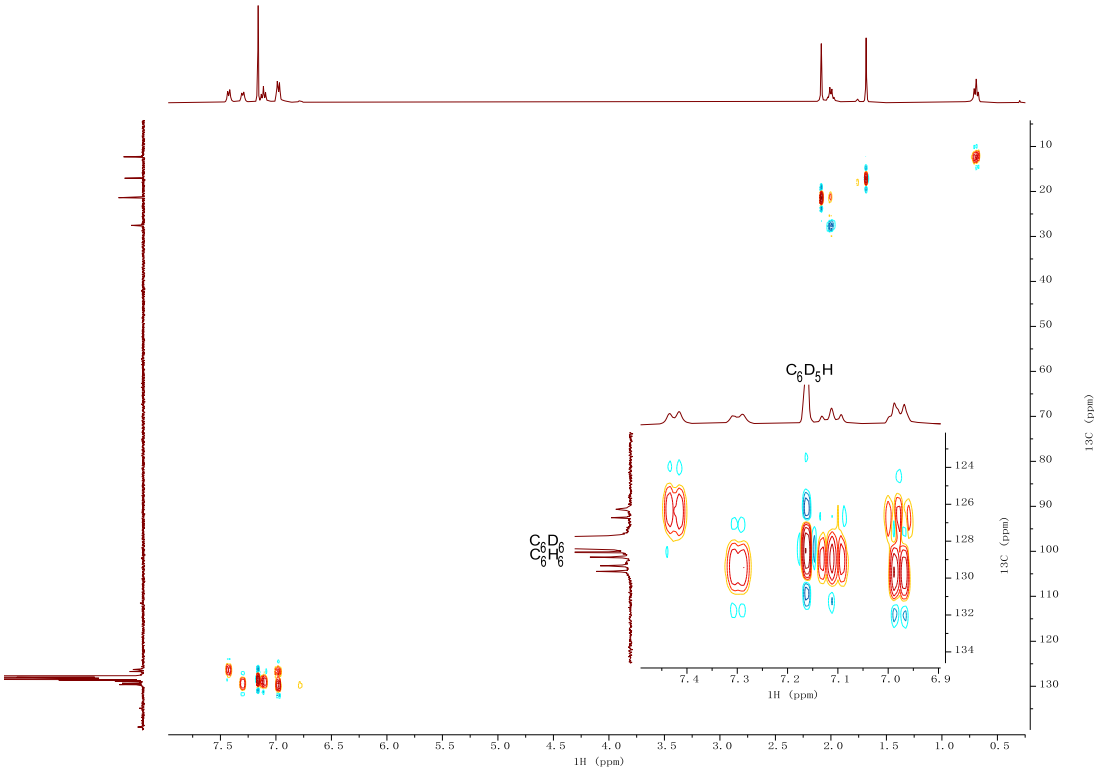

Figure S13. ^{1}H-^{13}C HSQC NMR spectrum of **1-dimer** in the C_6D_6 solution of the mixture.

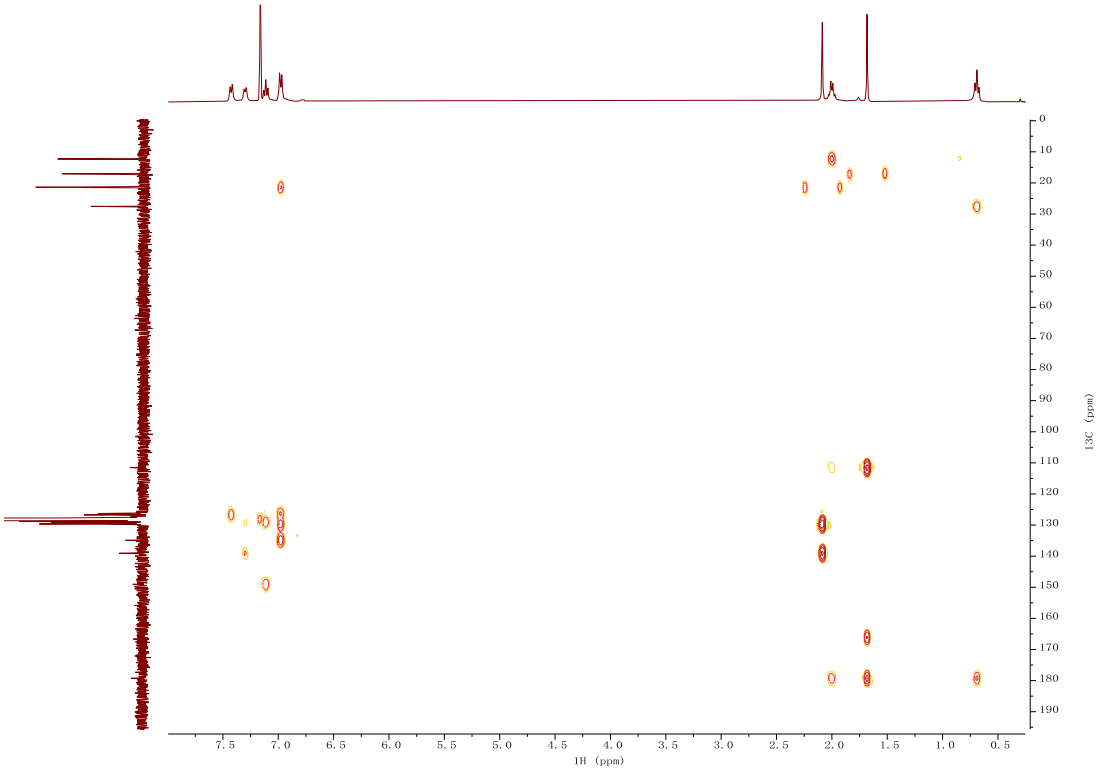

Figure S14. ^{1}H-^{13}C HMBC NMR spectrum of **1-dimer** in the C_6D_6 solution of the mixture.

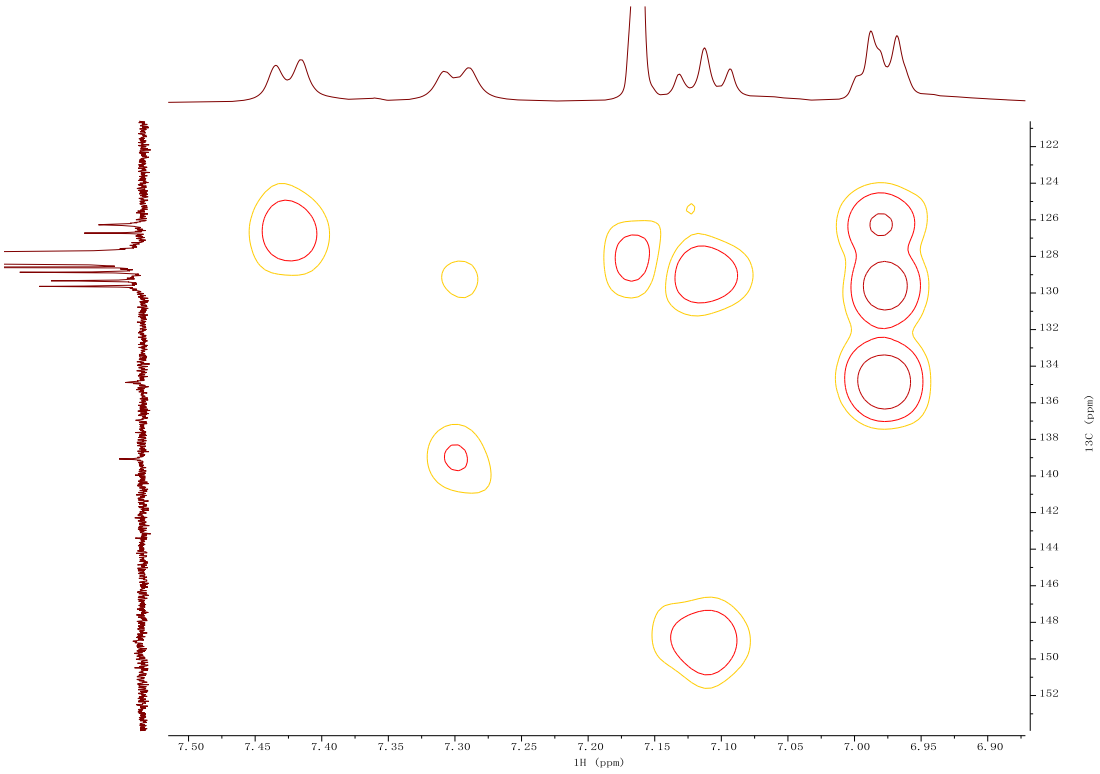

Figure S15. Aromatic region of ^{1}H-^{13}C HMBC NMR spectrum of **1-dimer** in the C_6D_6 solution of the

mixture.

TEMPO Oxidation of 1

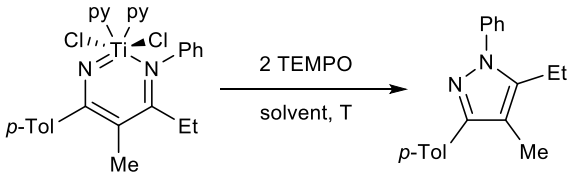

1 **2**

entry	solvent	T (˚C)	time (h)	yield (%)
1	C_6D_6	50	2	92
2	C_6D_6	35	5 (22)	61 (76)
3	C_6D_6	r.t.	2	29
4	CD_2Cl_2	50	5 (22)	77 (82)
5	1,2-$Cl_2C_2H_4$	50	2	99

Table S1. TEMPO oxidation of **1** under various conditions. Extended time reaction conditions and yields are noted in parentheses.

1 (5.5 mg, 0.01 mmol, 1.0 equiv), TEMPO (3.1 mg, 0.02 mmol, 2.0 equiv), internal standard (entries 1, 3, 5: TMB, 5.0 mg, 0.03 mmol; entries 2, 4: HMDSO, 0.008 mmol, in 0.01 mL stock solution in C_6D_6), and 0.5 mL solvent were added to an NMR tube in the glovebox. The NMR tube was capped and placed in the oil bath at corresponding temperature. ^{1}H NMR spectra were collected before and after the reaction. The reaction product **2** matched up with the reported chemical shifts.[1] The reaction yields were determined *via* ^{1}H NMR against the internal standard.

Example NMR spectra are listed below.

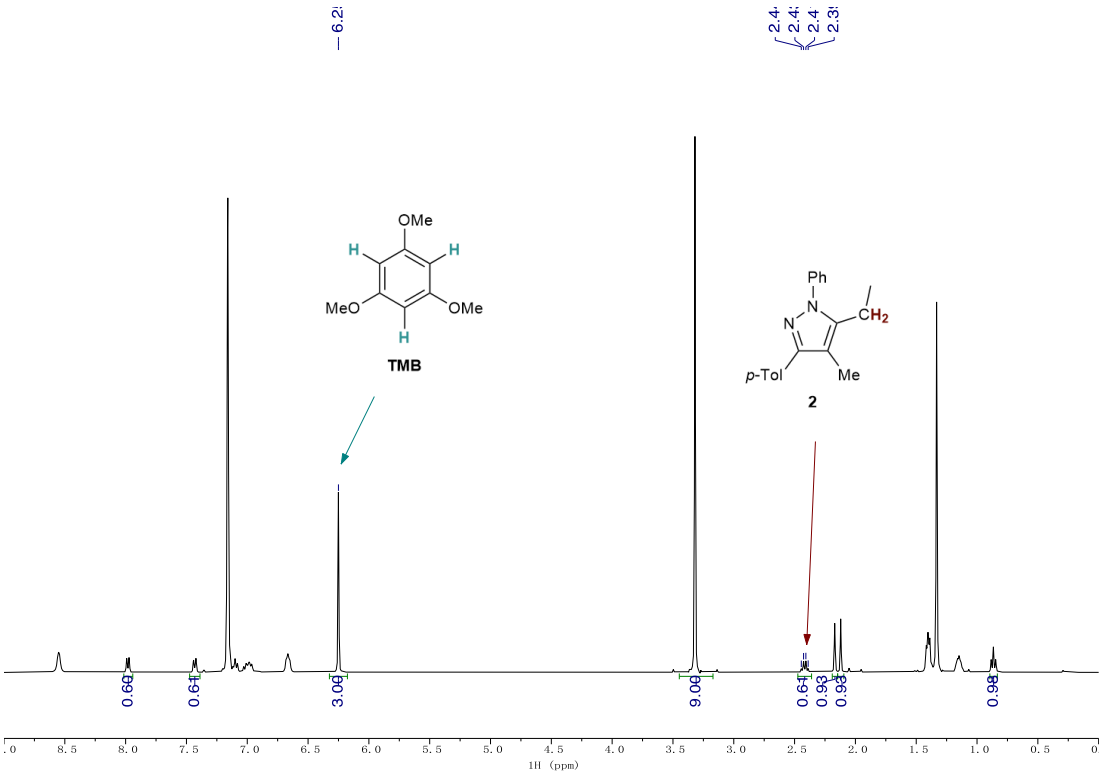

Figure S16. Time = 2 hours ^{1}H NMR spectrum of TEMPO oxidation of **1** in C_6D_6 at 50 ˚C (entry 1). Peaks for yield calculation are labelled with chemical shifts and structural assignments.

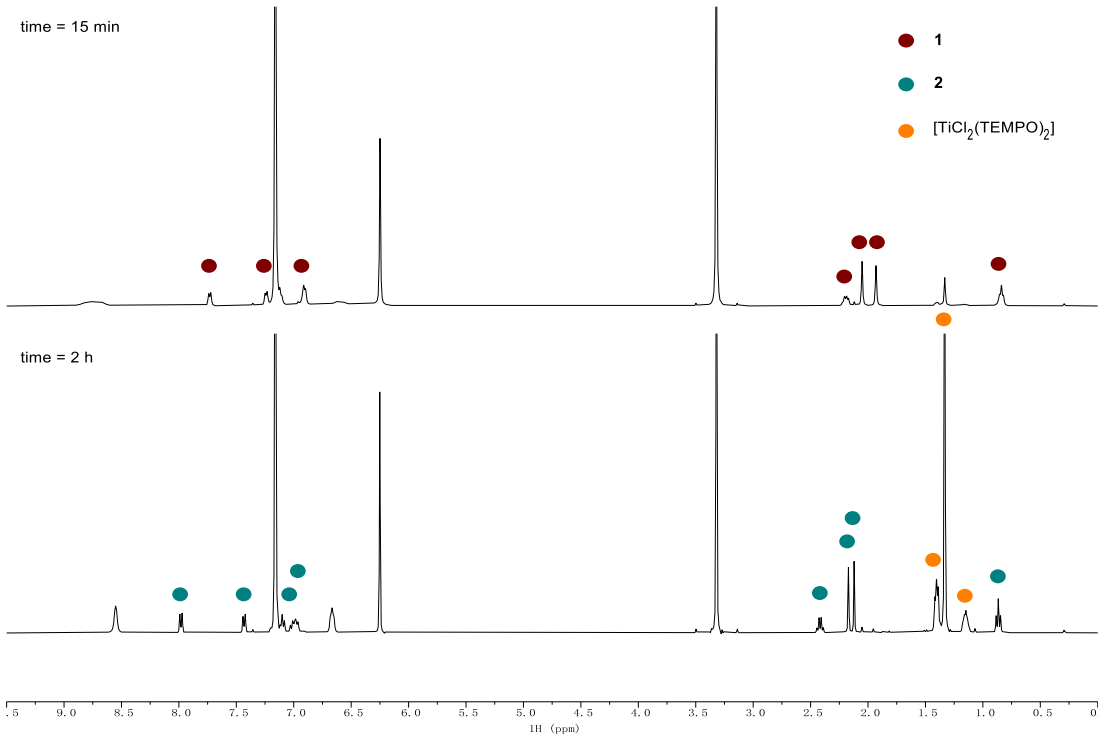

Figure S17. Stacked ^{1}H NMR spectra of TEMPO oxidation of **1** in C_6D_6 at 50 ˚C (entry 1). Top: time = 15

minutes. Bottom: time = 2 hours.

TEMPO Oxidation of 3

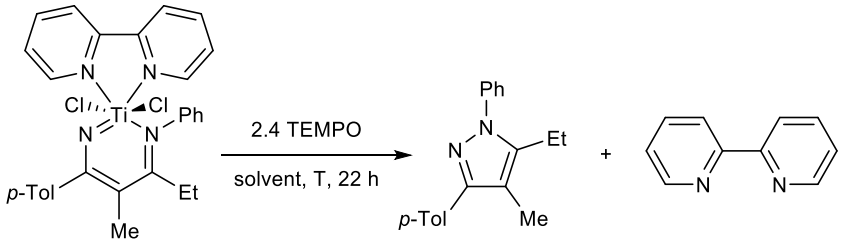

3 (5.5 mg, 0.01 mmol, 1.0 equiv), TEMPO (3.7 mg, 0.024 mmol, 2.4 equiv), TMB (5.0 mg, 0.03 mmol, internal standard), and 0.5 mL solvent (CH_2Cl_2 or 1,2-$Cl_2C_2H_4$) were added to an NMR tube in the glovebox. The NMR tube was capped and placed in the oil bath at corresponding temperature (50 ˚C or 90 ˚C) for 22 hours. ^{1}H NMR spectra were collected before and after the reaction. The reaction yields were determined *via* No-D ^{1}H NMR against the internal standard TMB.

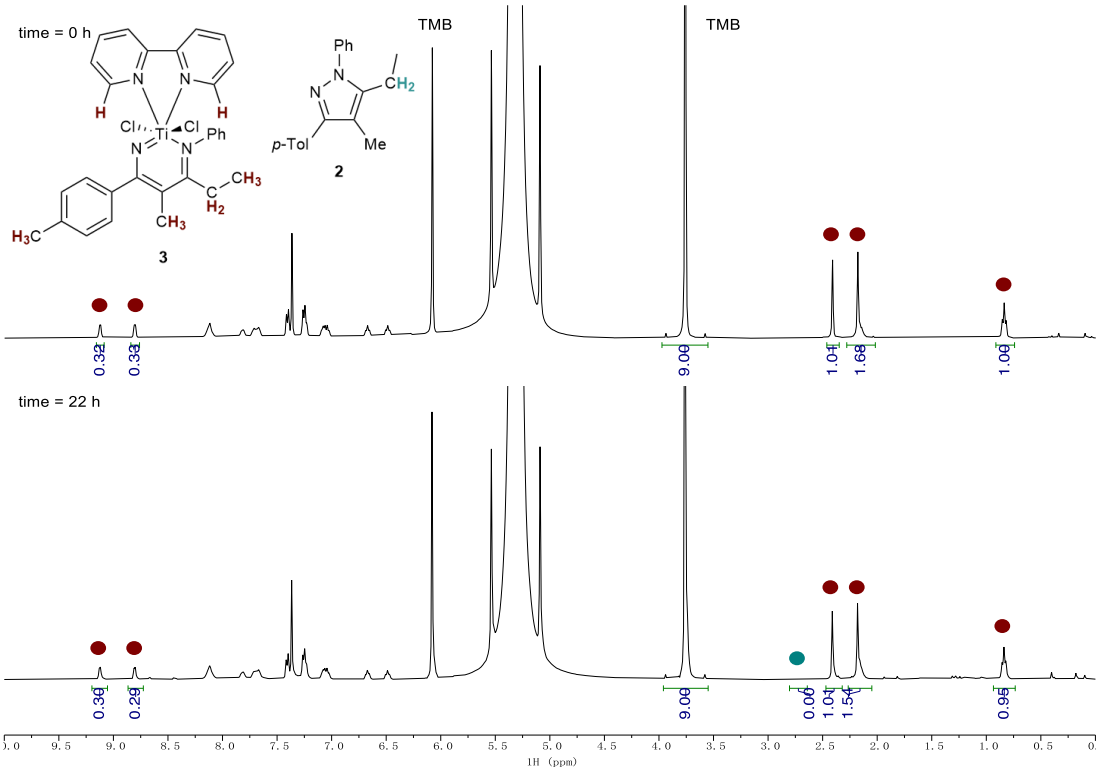

Figure S18. Stacked No-D ^{1}H NMR spectra of TEMPO oxidation of **3** in CH_2Cl_2 at 50 ˚C.

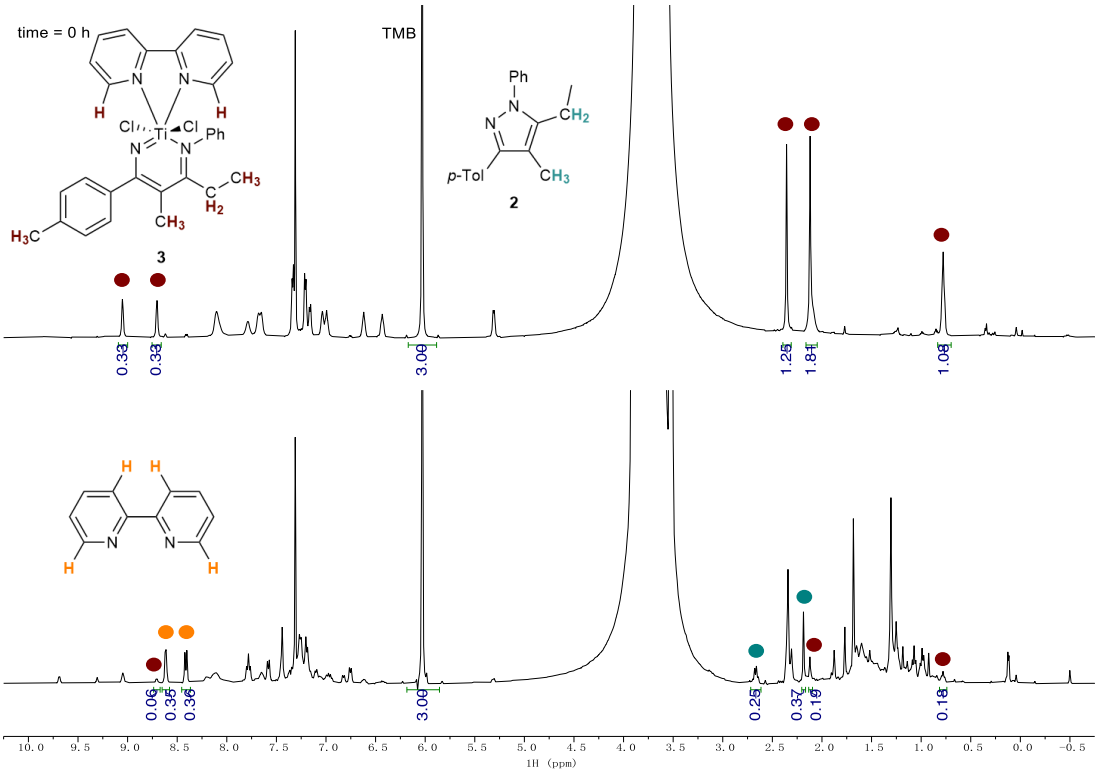

Figure S19. Stacked No-D ^{1}H NMR spectra of TEMPO oxidation of **3** in 1,2-$Cl_2C_2H_4$ at 90 ˚C.

TEMPO Oxidation of 1-dimer

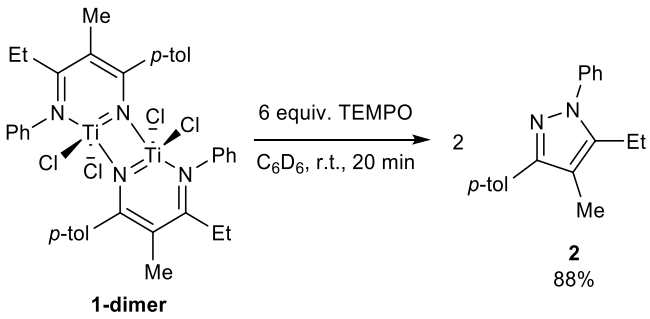

The product mixture solution in C_6D_6 from the reaction between **1** and $TiCl_4$ was diluted to 0.5 mL and added to an NMR tube in the glovebox. This solution contains **1-dimer** (0.0034 mmol, determined by ^{1}H NMR against internal standard, 1.0 equiv) and HMDSO (0.008 mmol). TEMPO (0.02 mmol, 6 equiv.) was added to the NMR tube before the tube was capped and shaken vigorously to ensure the thorough mixing. ^{1}H NMR was collected at 20 minutes. Due to the rapid reaction, time = 0 NMR was unable to be collected. Time = 30 minutes, 10 h and 20 h NMR spectra were also collected, while only minor changes have been observed. The reaction product **2** matched up with the reported chemical shifts.[1] The reaction yields were determined *via* ^{1}H NMR against the internal standard HMDSO.

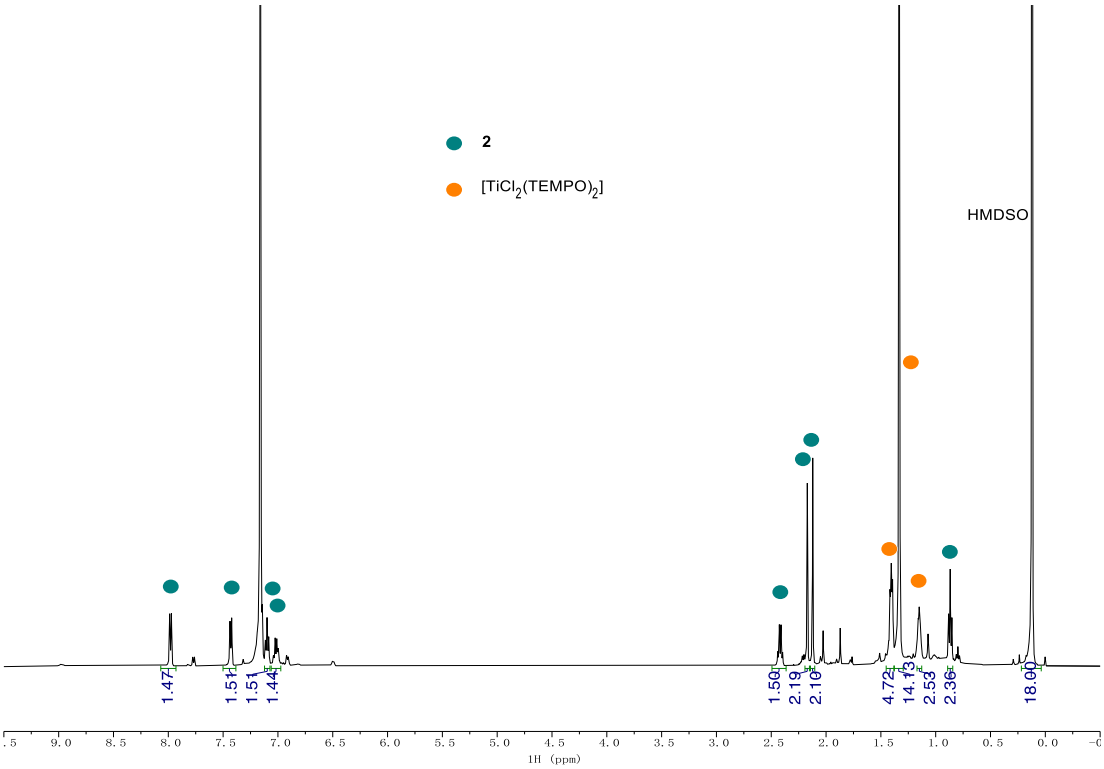

Figure S20. Time = 20 minutes ^{1}H NMR spectrum of TEMPO oxidation of **1-dimer** in C_6D_6.

FcCl Oxidation of 1 and 3

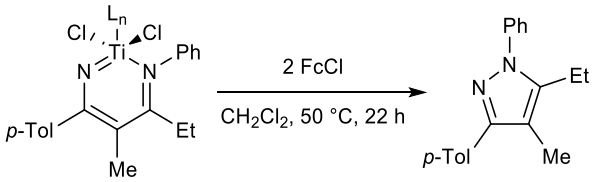

2

L_n = 2 py (**1**) 50%
bpy (**3**) 11%

1 or **3** (0.01 mmol, 1.0 equiv), ferrocenium chloride (FcCl, 4.4 mg, 0.02 mmol, 2 equiv), 0.5 mL CH_2Cl_2, and a stir bar were added to a 4 mL scintillation vial in the glovebox. The vial was capped and heated at 50 ˚C for 22 hours. TMB (1.7 mg, 0.01 mmol, internal NMR standard) was added after the reaction mixture cooled down to room temperature and taken out of the glovebox. The reaction yield was determined *via* No-D ^{1}H NMR in CH_2Cl_2 against the internal standard TMB.

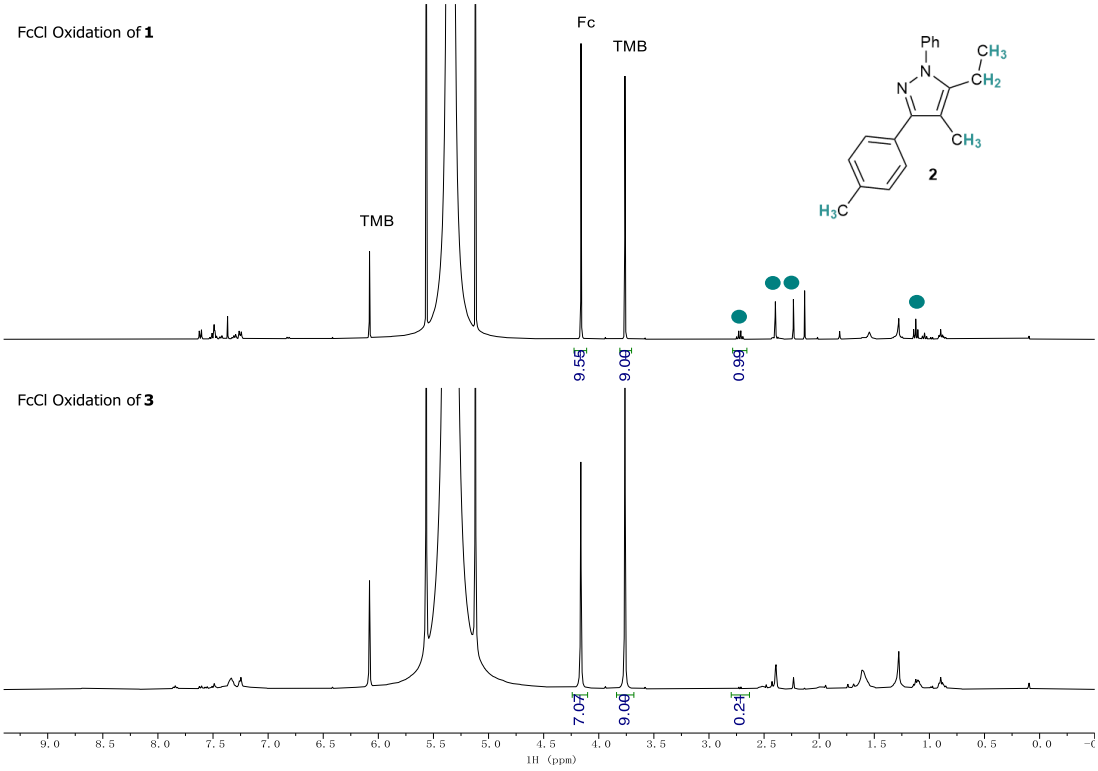

Figure S21. Stacked No-D ^{1}H NMR spectra of FcCl oxidation of (top) **1** and (bottom) **3** in CH_2Cl_2 after the addition of TMB.

FcBArF Oxidation of 1 and 3

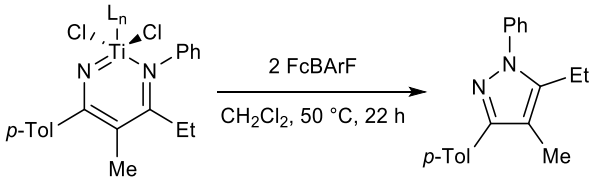

2

L_n = 2 py (**1**) *not observed*
bpy (**3**) *not observed*

1 or **3** (0.01 mmol, 1.0 equiv), ferrocenium BArF salt (FcBArF, BArF = tetrakis(3,5-bis(trifluoromethyl)phenyl)borate, 21.0 mg, 0.02 mmol, 2 equiv), 0.5 mL CH_2Cl_2, and a stir bar were added to a 4 mL scintillation vial in the glovebox. The vial was capped and heated at 50 °C for 22 hours. TMB (1.7 mg, 0.01 mmol, internal NMR standard) was added after the reaction mixture cooled down to room temperature and taken out of the glovebox. The reaction mixture was then extracted between CH_2Cl_2/H_2O. The organic phase was evaporated after being dried over $MgSO_4$. The reaction yield was determined *via* ^{1}H NMR in C_6D_6 against the internal standard TMB.

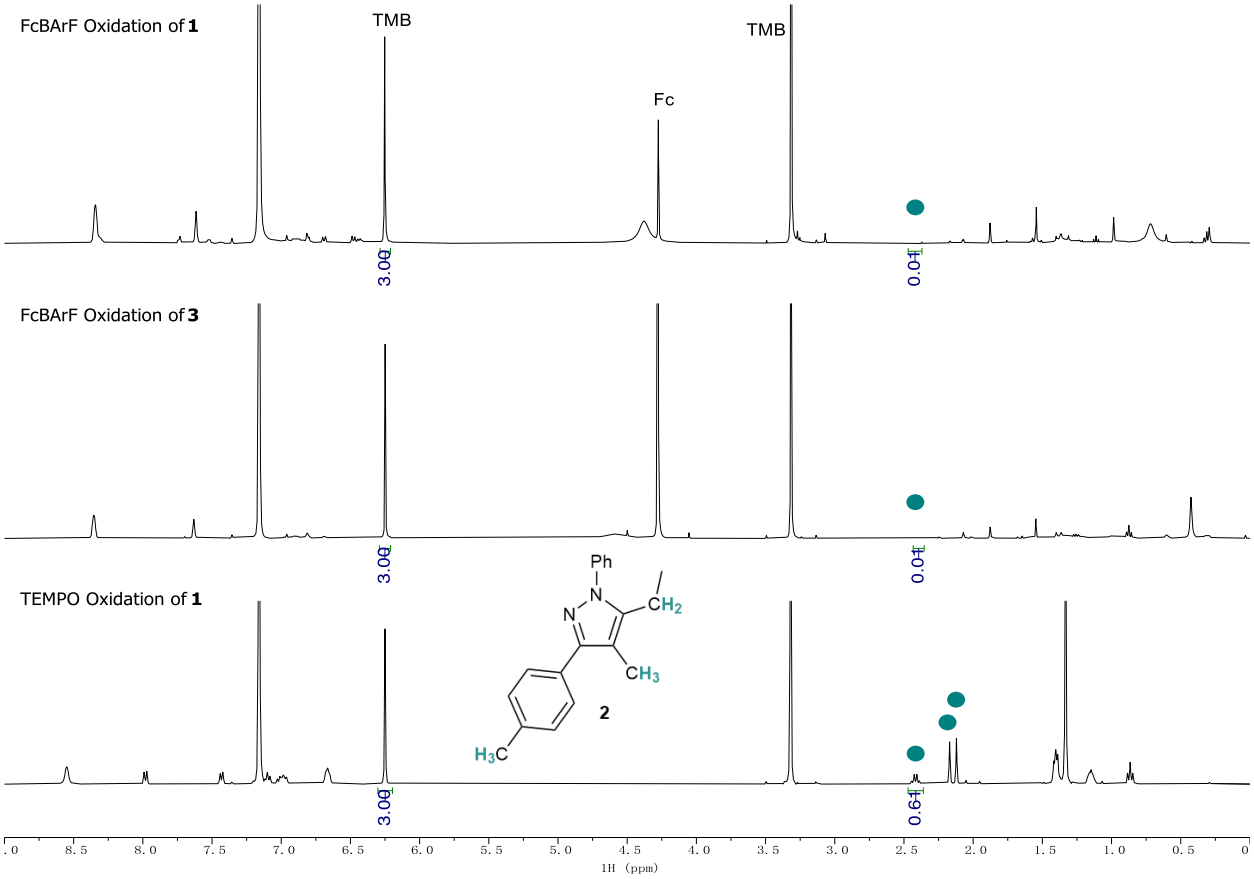

Figure S22. Stacked ^{1}H NMR spectra of FcBArF oxidation of (top) **1** and (middle) **3** in C_6D_6 after aqueous workup, and (bottom) TEMPO oxidation of **1** (Table S1 entry 1) in C_6D_6 as a comparison.

Oxidation of 1 with $(NEt_4)_2CeCl_6$

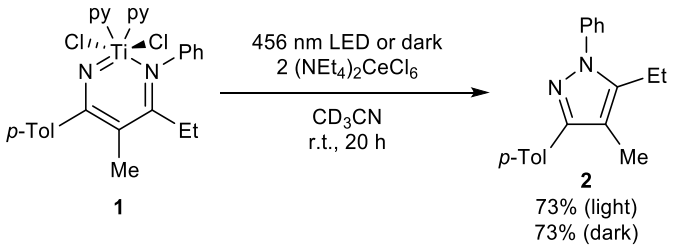

1 (13.8 mg, 0.025 mmol, 1.0 equiv), $(NEt_4)_2CeCl_6$ (30.7 mg, 0.05 mmol, 2.0 equiv), TMB (5.0 mg, 0.03 mmol, internal standard), 0.5 mL CD_3CN, and a stir bar were added to a 4 mL scintillation vial in the glovebox. The vial was capped, taken out of the glovebox, and stir in the dark at room temperature for 20 hours. The reaction mixture was then transferred into an NMR tube in the glovebox, and the reaction yield was determined *via* ^1H NMR against the internal standard TMB.

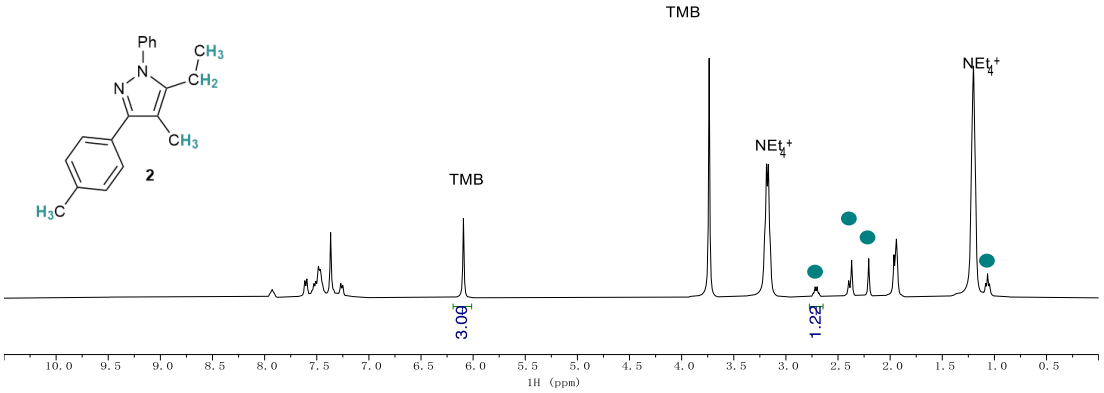

Figure S23. ^1H NMR spectrum of $(NEt_4)_2CeCl_6$ oxidation of **1** in CD3CN.

Standard Procedure for ^1H NMR Monitoring Kinetic Studies

TEMPO oxidation of **1** at room temperature (Table S1, entry 3) revealed that **1** could undergo Ti-mediated pyrazole synthesis with TEMPO slowly without heating. To obtain the optimal t = 0 data, cooling was applied to the reaction mixture to decelerate this reaction before the measurement took place.

Standard Procedure:

J-Young NMR tube was cooled in a pre-cooled cold well (coolant: dry ice/acetone) in the glovebox for 30 minutes. C_6D_6 stock solution of **1** (0.020 mol/L), HMDSO (internal standard, 50 µL, 0.008 mol/L), and TEMPO (0.160 mol/L) were added with syringe in order. The solution was immediately frozen due to the low temperature of the pre-cooled J-Young NMR tube and high melting point of C_6D_6, preventing **1** from reacting with TEMPO prior to the NMR monitoring experiment. C_6D_6 was further added till the volume of the reaction solution was 400 µL. The NMR tube was capped, quickly taken out of the glovebox, and immediately cooled in an ice water bath. The reaction mixture was kept frozen during the temperature calibration of the NMR spectrometer. Shimming was performed on a C_6D_6 solution of **1**. When switching to samples for monitoring experiments, shimming was not performed again in order to shorten the time interval between t = 0 and the 1st acquisition. Before the measurement, the NMR tube was taken out of the ice water bath, allowed to warm up in a 35 ˚C bath for 20 seconds, shaken to mix the reactants, and injected

into the NMR spectrometer. A timer was started when the NMR tube was taken out of the ice water bath to obtain a relatively accurate t = 0 time point. Multiple acquisitions were performed in automatic mode in 30 seconds interval (dummy scan = 0, number of scan = 1, acquisition time = 5 s, delay = 20 s, idle time = 5 s). The ^{1}H NMR spectra were processed using batch integration (MestReNova, integrals graph). The concentration of **1** and **2** were obtained from their peak integrals against the peak integral of HMDSO.

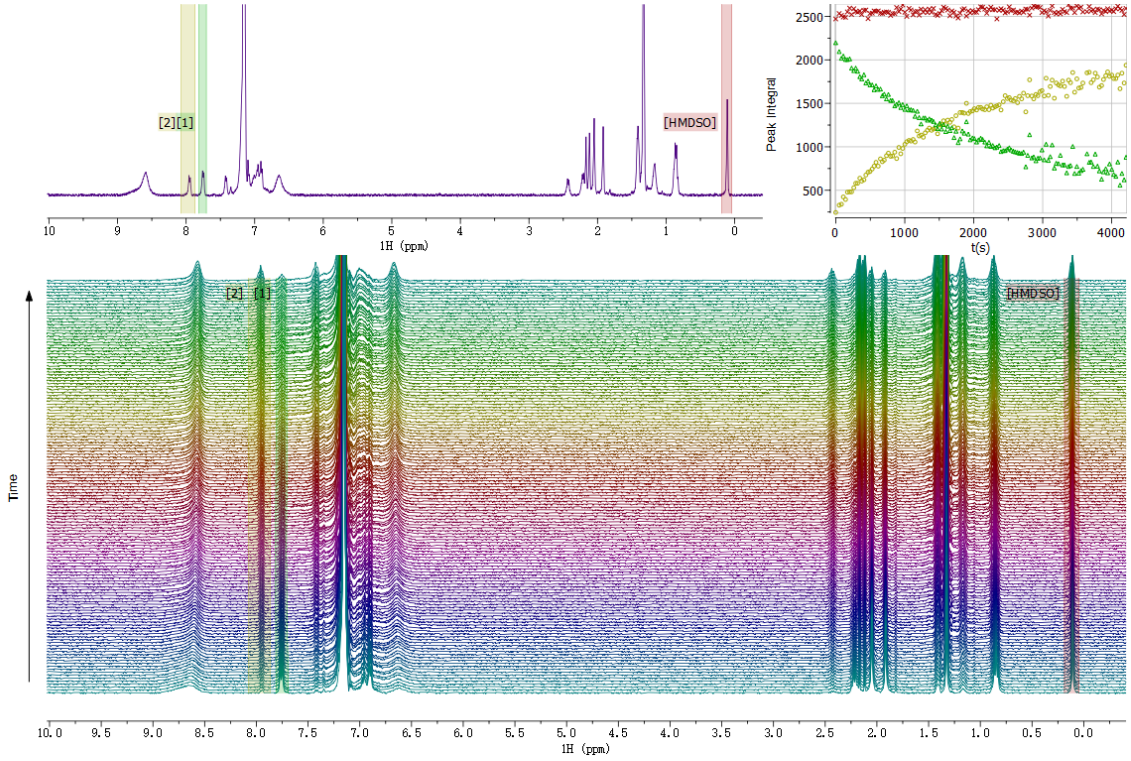

Figure S24. Process of example ^{1}H NMR kinetic trace from entry 1, Table SXXX. (Top left) spectrum of an example time point (the 38th time point is shown in the spectrum). (Top right) peak integral versus time plot of HMDSO (red trace), **1** (green trace), and **2** (yellow trace). (Bottom) stacked spectra of the kinetic trace with batch integration of HMDSO, **1** and **2**.

Time Adjustment Experiment and Analysis

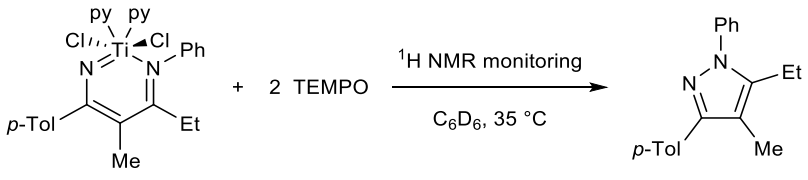

entry	[**1**] (mol/L)	[TEMPO] (mol/L)
1	0.010	0.020
2	0.006	0.012

Table S2. Conditions of the time adjustment experiment.

The measurements were performed following **Standard Procedure** under the conditions in the table

above. The consumption of **1** was monitored *via* ^{1}H NMR, and the concentration of **1** was plotted against reaction time. "Time adjusted" trace of entry 2 was obtained by plotting the consumption profile in entry 2 against an adjusted time profile (t' = t + 1600, in seconds) to allow the starting coordinate of the "time adjusted" trace locates on the trace of entry 1. The overlap of the trace of entry 1 and the "time adjusted" trace suggested that product inhibition and side reactions are kinetically insignificant in this reaction system.

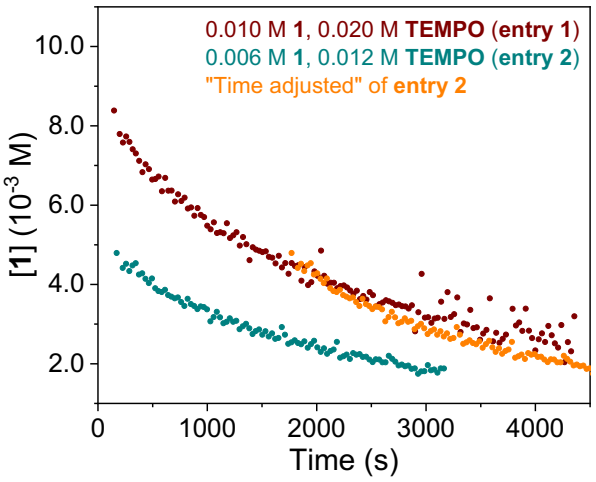

Figure S25. Concentration of **1** vs. time plots of entries 1, 2, and "time adjusted".

Variable Time Normalization Analysis on 1

Variable time normalization analysis (VTNA) with varied concentration of **1** was performed for determination of reaction order of **1**:

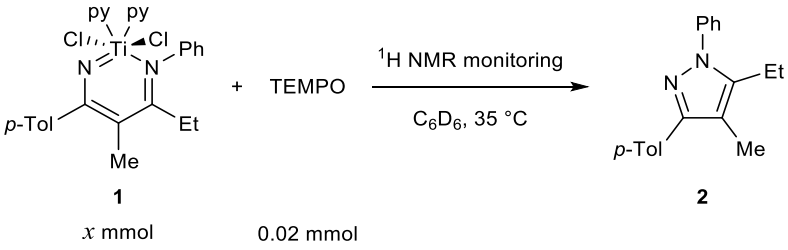

entry	[**1**] (mol/L)	[TEMPO] (mol/L)
1	0.010	0.020
2	0.0075	0.020
3	0.005	0.020

Table S3. Conditions of the VTNA experiments for reaction order of **1**.

The measurements were performed following **Standard Procedure** under the conditions in the table above. The formation of **2** was monitored *via* ^{1}H NMR. The concentration of **2** (approximated via the trapezoid rule) was plotted against an adjusted time scale $\sum[\mathbf{1}]^{\alpha}\Delta t$ with

$$\sum [\mathbf{1}]^{\alpha} \Delta t = \sum_{i=1}^{n} \left(\frac{[\mathbf{1}]_i + [\mathbf{1}]_{i-1}}{2} \right)^{\alpha} (t_i - t_{i-1})$$

where α is the order of dependence on **1** and t is the reaction time.[5–7] The reaction order of **1** was obtained by adjusting α to allow the kinetic traces of entries 1-3 visually overlapped. α = 0.7 was found to give the best overlapped of the kinetic traces. Three characteristic VTNA plots (α = 0, 0.5, 0.7, 1) and the raw data in [**2**] versus time plot are shown below.

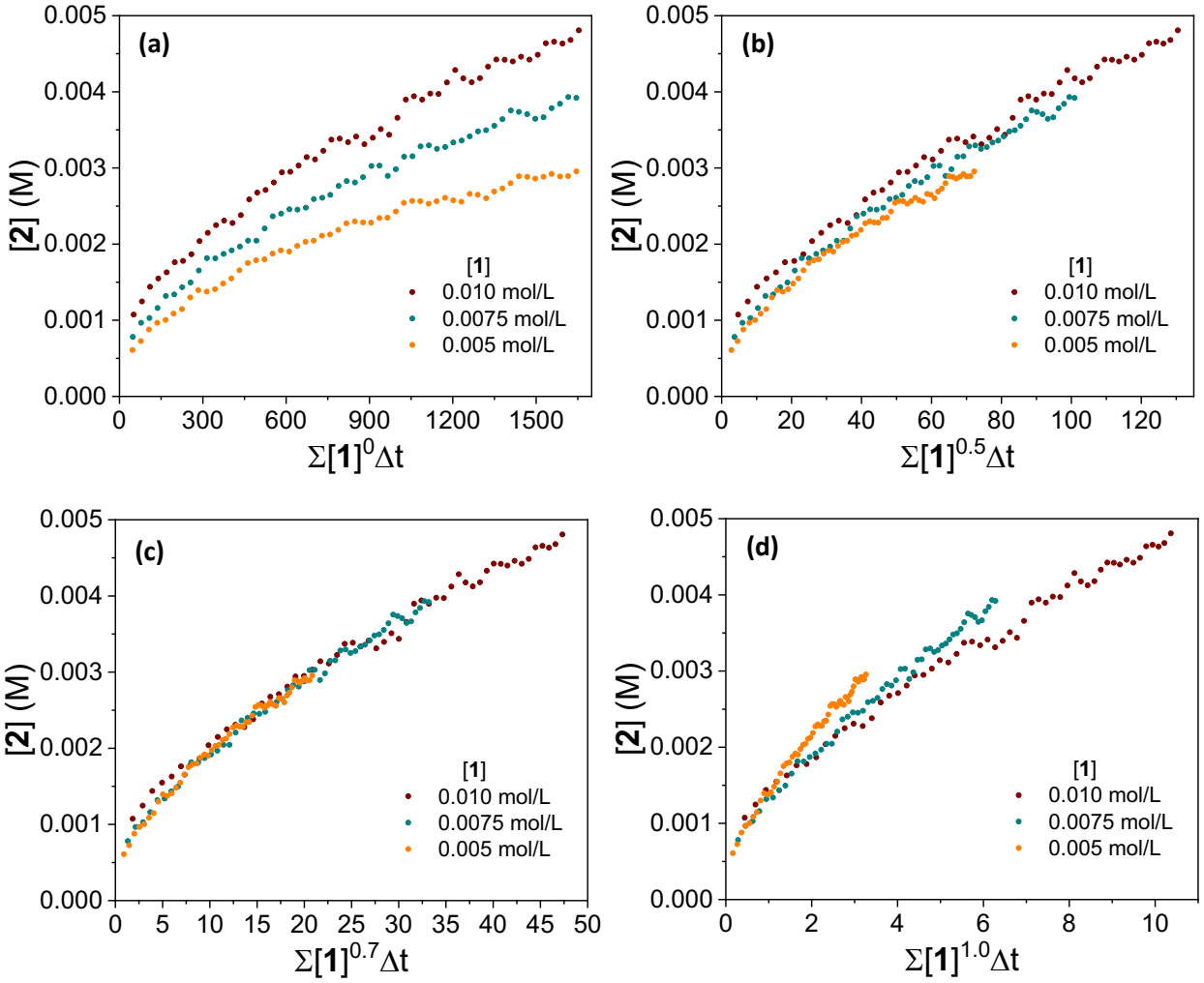

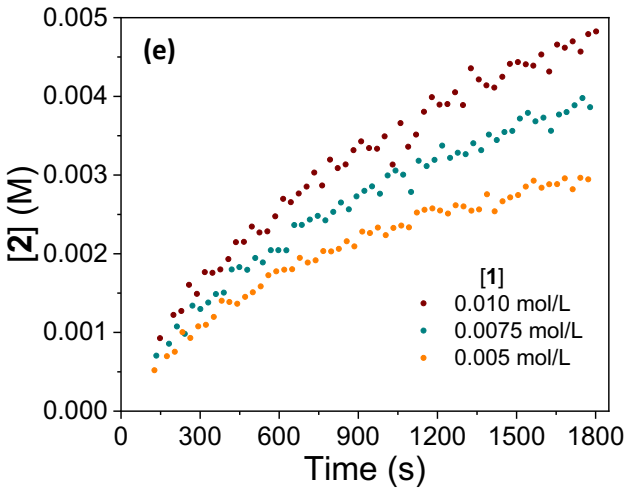

Figure S26. VTNA plots with α = (a) 0, (b) 0.5, (c) 0.7, (d) 1, and (e) the raw data in [**2**] versus time plot.

Variable Time Normalization Analysis on Pyridine

VTNA with varied concentration of pyridine was performed for determination of reaction order of pyridine:

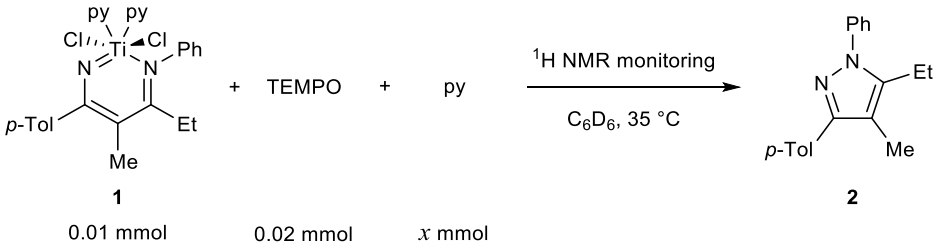

entry	[**1**] (mol/L)	[TEMPO] (mol/L)	[py] (mol/L)
1	0.010	0.020	0
2	0.010	0.020	0.004
3	0.010	0.020	0.010

Table S4. Conditions of the VTNA experiments for reaction order of pyridine.

The measurements were performed following **Standard Procedure** under the conditions in the table above. The formation of **2** was monitored *via* ^{1}H NMR. The concentration of pyridine (noted as [py]) was monitored *via* ^{1}H NMR. The concentration of **2** (approximated via the trapezoid rule) was plotted against an adjusted time scale $\sum[py]^{\alpha}\Delta t$ with

$$\sum[py]^{\alpha}\Delta t = \sum_{i=1}^{n}\left(\frac{[py]_i + [py]_{i-1}}{2}\right)^{\alpha}(t_i - t_{i-1})$$

where α is the order of dependence on pyridine and t is the reaction time.[5–7] The reaction order of pyridine was obtained by adjusting α to allow the kinetic traces of entries 1-3 visually overlapped. α = -2.5 was found to give the best overlapped of the kinetic traces. Three characteristic VTNA plots (α = 0, -1, -2, -2.5, -3) and the raw data in [**2**] versus time plot are shown below.

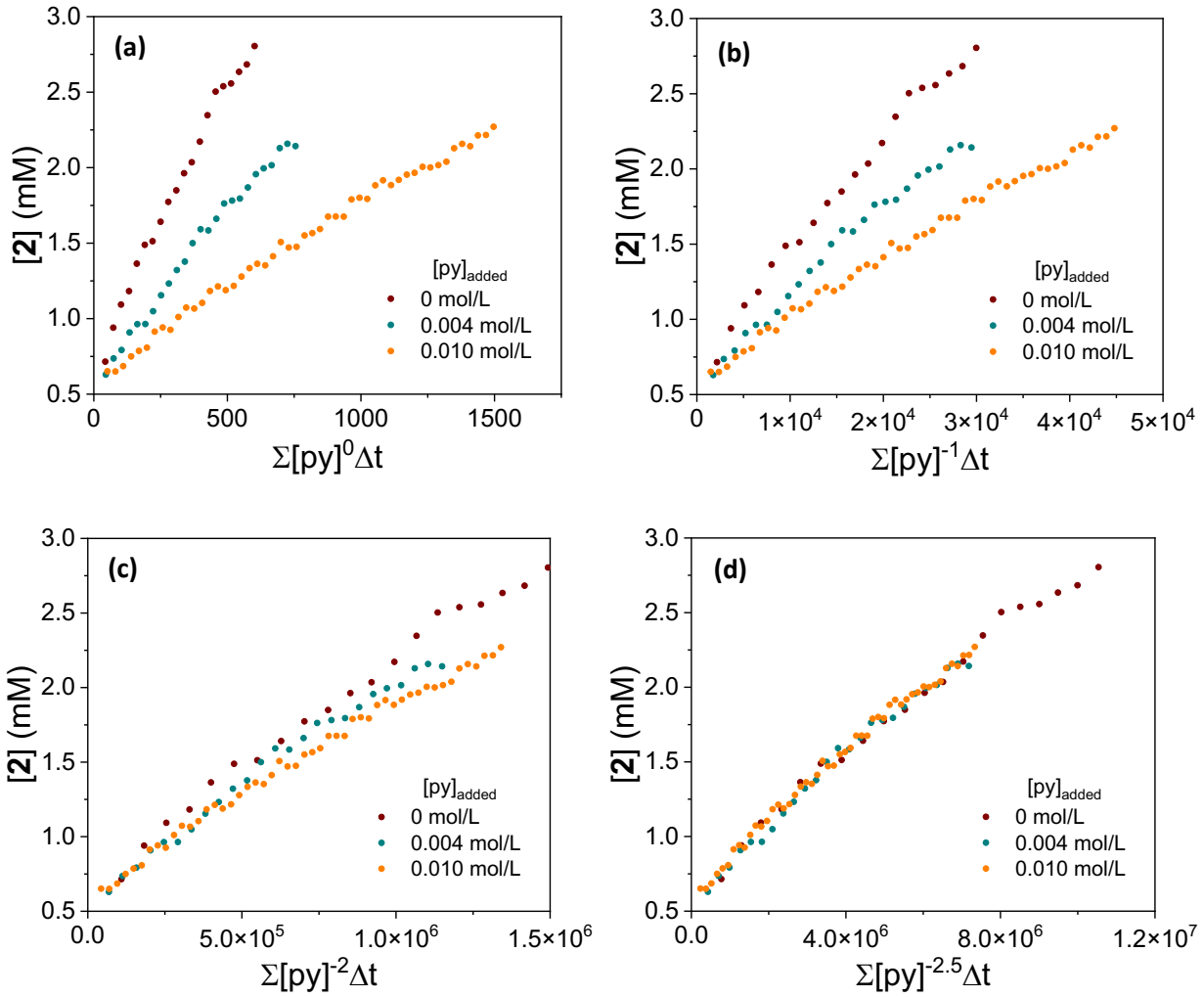

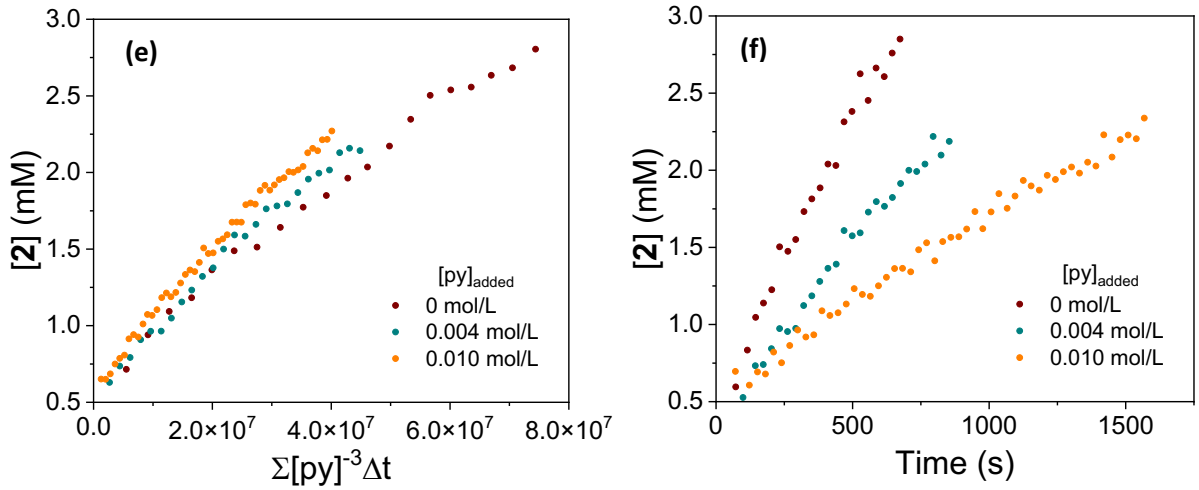

Figure S27. VTNA plots with α = (a) 0, (b) -1, (c) -2, (d) -2.5, (e) -3, and (f) the raw data in [**2**] versus time plot.

Initial Rate Measurements on TEMPO

Initial rate measurement with varied concentration of TEMPO for determination of reaction order of TEMPO:

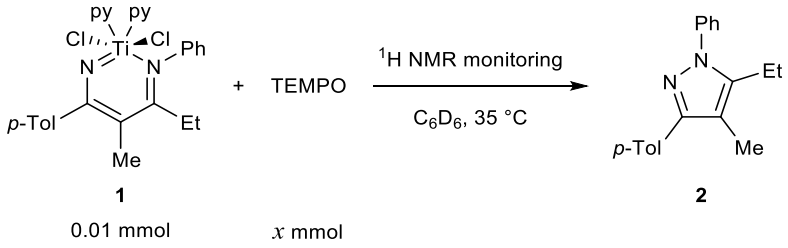

entry	[**1**] (mol/L)	[TEMPO] (mol/L)	(d[**2**]/dt)$_{int}$ (10^{-6} mol/(L*s))
1	0.010	0.020	4.51281
2	0.010	0.016	4.27914
3	0.010	0.020	4.43008
4	0.010	0.020	4.00074
5	0.010	0.012	3.38525
6	0.010	0.008	2.04410
7	0.010	0.004	1.23593
8	0.010	0.024	5.13483
9	0.010	0.028	5.84779
10	0.010	0.024	4.99294
11	0.010	0.016	3.30507
12	0.010	0.012	2.91090
13	0.010	0.008	2.15967
14	0.010	0.004	1.01667
15	0.010	0.028	5.53663
16	0.010	0.028	6.92910

17	0.010	0.024	5.27840
18	0.010	0.016	3.30628
19	0.010	0.012	2.49613

Table S5. Conditions and results of the initial rates measurement for reaction order of TEMPO.

The measurements were performed following **Standard Procedure** under the conditions in the table above. The formation of **2** was monitored *via* ^{1}H NMR. The concentration of **2** was plotted against reaction time. Initial rates of the formation of **2**, known as $d[\mathbf{2}]/dt)_{int}$, were obtained from the slope of the linear function fitting curve of each entry. $d[\mathbf{2}]/dt)_{int}$ was then plotted against [TEMPO], and the experimental reaction order of TEMPO can be obtained from the power function fitting of the plot as 0.87.

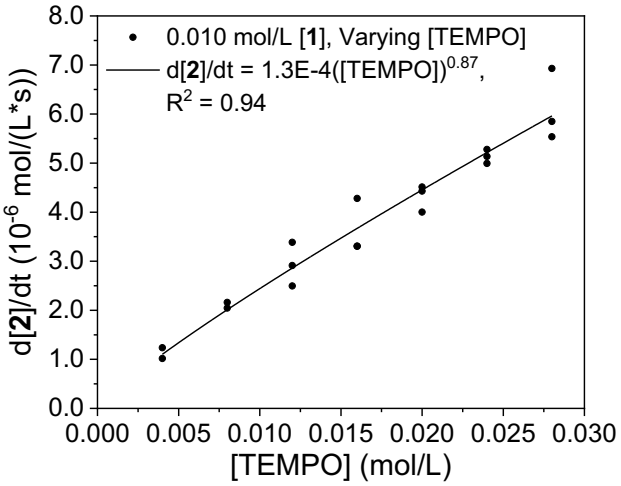

Figure S28. Initial rates versus concentrations of TEMPO plot and the power fitting result.

Cyclic Voltammetry

Cyclic voltammetry of **1** was collected in CH_2Cl_2 with 0.1 M TBABArF as electrolyte at scan rate = 200 mV/s. Fc was used as potential reference which was then converted to SCE based on reported $Fc^{0/+}$ couple vs. SCE in CH_2Cl_2.[8]

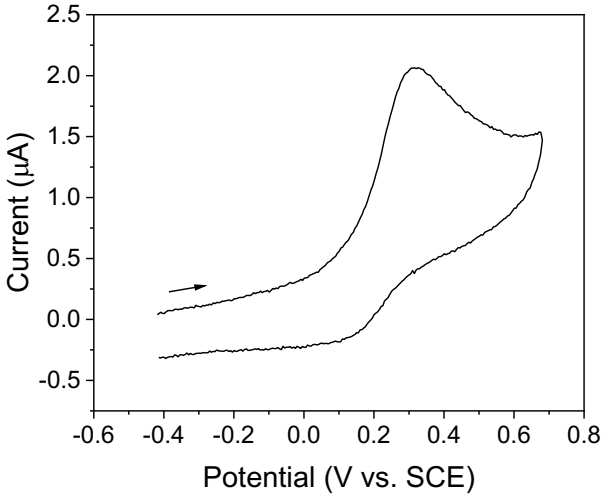

Figure S29. Cyclic voltammetry of **1** in CH_2Cl_2 with 0.1 M TBABArF.

DOSY of 1 and 1-dimer

DOSY NMR spectra were collected with first gradient amplitude = 2%, final gradient amplitude = 98%, number of points = 19 and linear ramp type. DOSY transformation was performed using Bayesian method with resolution factor = 1 and repetitions = 2. Estimated molecular weight (MW) was obtained by subjecting the diffusion coefficient (*D*) from DOSY spectra to SEGWE calculator (Manchester NMR Methodology Group, https://nmr.chemistry.manchester.ac.uk/?q=node/432).[9,10] DOSY spectra of **1** were collected at two concentrations: (1) 0.010 mol/L **1** in C_6D_6 and (2) 0.003 mol/L **1** in C_6D_6. DOSY spectrum of **1-dimer** was collected from a C_6D_6 solution diluted from the product solution mixture from the reaction between **1** and $TiCl_4$, which contained 0.010 mol/L **1-dimer** in C_6D_6. DOSY of **3** was not collected due to the low solubility of **3** in C_6D_6. **3** is soluble CD_2Cl_2, however the estimated MW of **3** based on its DOSY in CD_2Cl_2 was inaccurate due to the low viscosity of CD_2Cl_2.

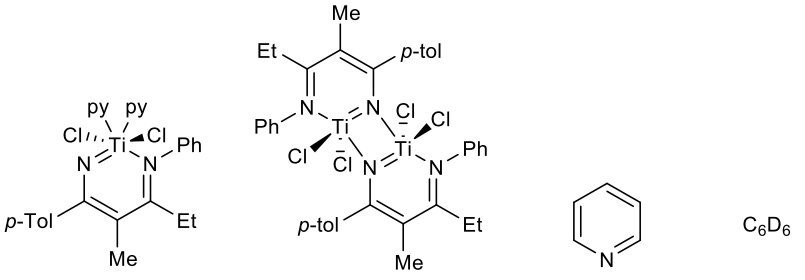

Figure S30. Proposed species found in DOSY studies and their MW.

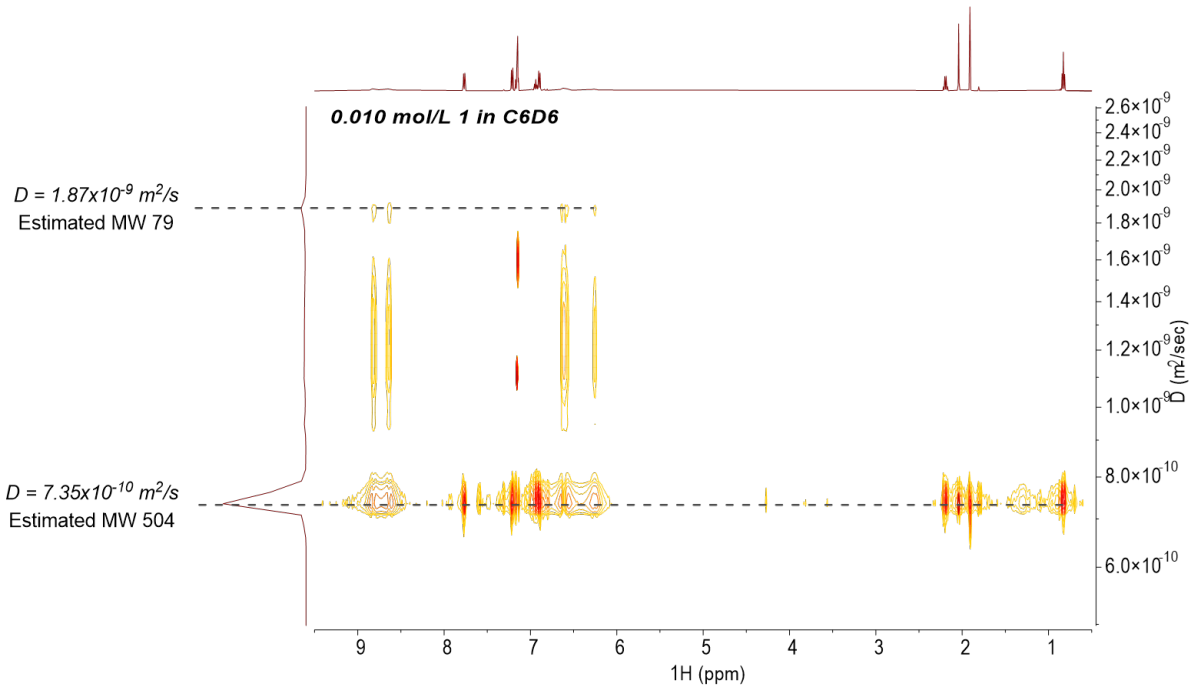

Figure S31. DOSY NMR spectrum of 0.010 mol/L **1** in C_6D_6.

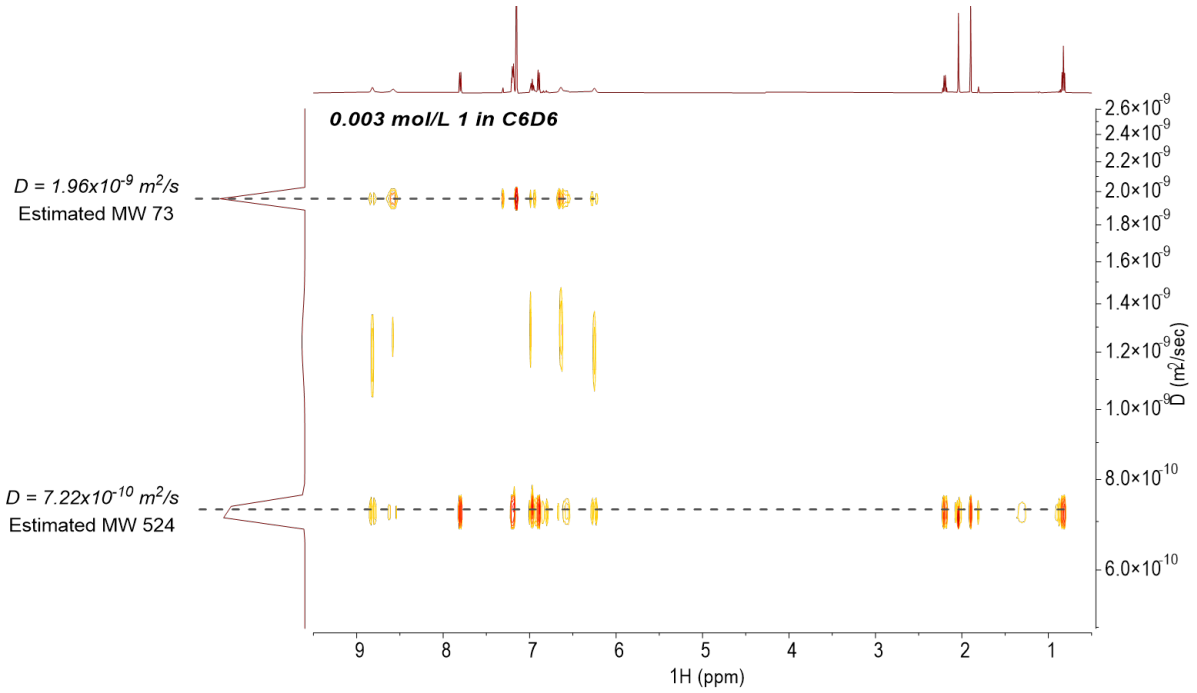

Figure S32. DOSY NMR spectrum of 0.003 mol/L **1** in C_6D_6.

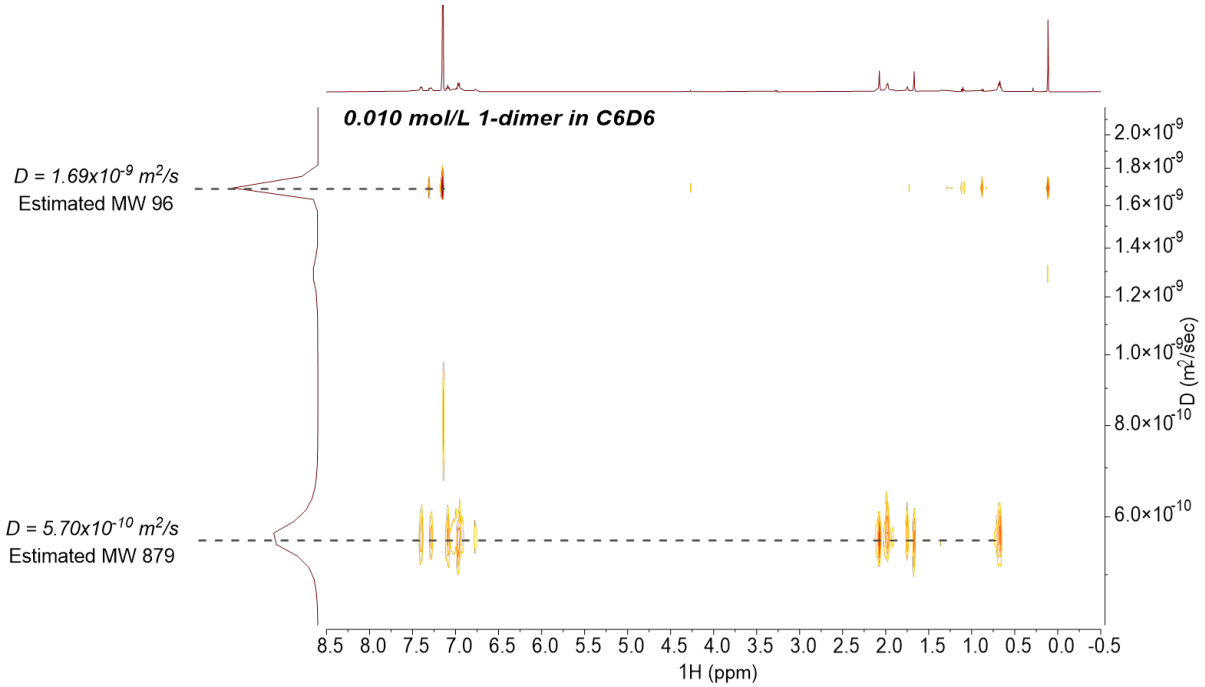

Figure S33. DOSY NMR spectrum of 0.010 mol/L **1-dimer** in C_6D_6.

XRD Data of 1-dimer

	1-dimer
CCDC Number	2348539
Empirical Formula	$C_{38}H_{40}Cl_4N_4Ti_2$
Formula Weight	790.34
Temperature (K)	150.0
a, Å	9.3405(9)
b, Å	9.3839(7)
c, Å	21.029(2)
α, °	90
β, °	90.745(2)
γ, °	90
Volume, Å^3	1843.0(3)
Z	2
Crystal System	Monoclinic
Space Group	$P2_1/c$
d_{calc}, g/cm^3	1.424
θ Range, °	1.937 to 30.617
μ, mm^{-1}	0.757
Abs. Correction	Multi-scan
GOF	1.130
R_1[a]	0.0375
wR_2[b] [I>2σ(I)]	0.0863

[a] $R_1 = \Sigma||F_o|-|F_c||/\Sigma|F_o|$. [b] $wR_2 = [\Sigma[w(F_o^2-F_c^2)^2]/\Sigma[w(F_o^2)^2]^{1/2}$.

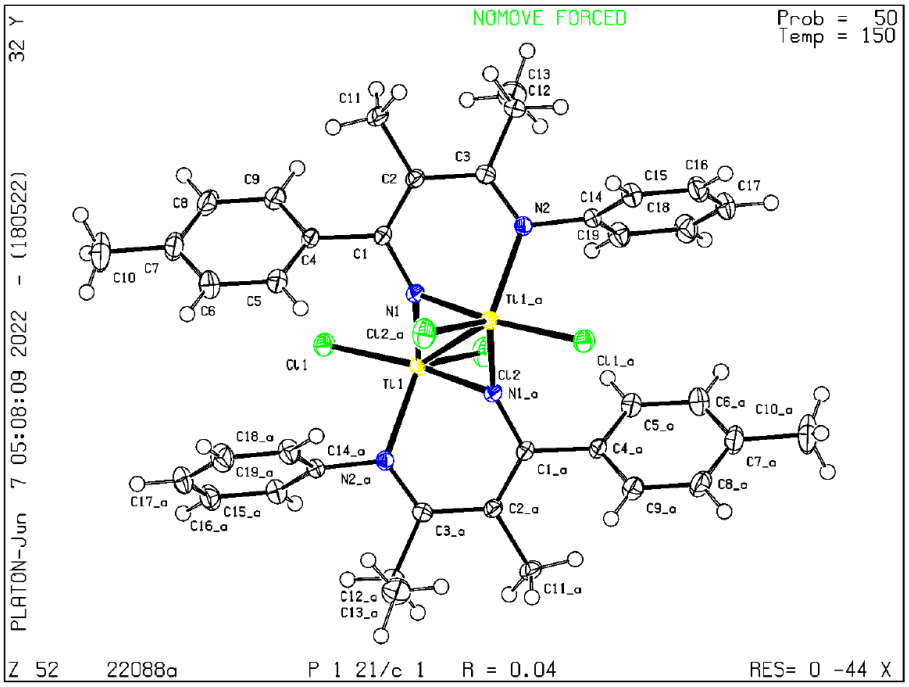

Figure S34. ORTEP diagram of **1-dimer**. Thermal ellipsoids are drawn at 50% probability.

Reference

(1) Pearce, A. J.; Harkins, R. P.; Reiner, B. R.; Wotal, A. C.; Dunscomb, R. J.; Tonks, I. A. Multicomponent Pyrazole Synthesis from Alkynes, Nitriles, and Titanium Imido Complexes via Oxidatively Induced N–N Bond Coupling. *J. Am. Chem. Soc.* **2020**, *142* (9), 4390–4399.

(2) Adams, J. J.; Arulsamy, N.; Sullivan, B. P.; Roddick, D. M.; Neuberger, A.; Schmehl, R. H. Homoleptic Tris-Diphosphine Re(I) and Re(II) Complexes and Re(II) Photophysics and Photochemistry. *Inorg. Chem.* **2015**, *54* (23), 11136–11149.

(3) Le Bras, J.; Jiao, H.; Meyer, W. E.; Hampel, F.; Gladysz, J. . Synthesis, Crystal Structure, and Reactions of the 17-Valence-Electron Rhenium Methyl Complex [(H5-C5Me5)Re(NO)(P(4-C6H4CH3)3)(CH3)]+ B(3,5-C6H3(CF3)2)4−: Experimental and Computational Bonding Comparisons with 18-Electron Methyl and Methylidene Complexes. *J. Organomet. Chem.* **2000**, *616* (1–2), 54–66.

(4) Löble, M. W.; Keith, J. M.; Altman, A. B.; Stieber, S. C. E.; Batista, E. R.; Boland, K. S.; Conradson, S. D.; Clark, D. L.; Lezama Pacheco, J.; Kozimor, S. A.; et al. Covalency in Lanthanides. An X-Ray Absorption Spectroscopy and Density Functional Theory Study of LnCl6x − (x = 3, 2). *J. Am. Chem. Soc.* **2015**, *137* (7), 2506–2523.

(5) Davis-Gilbert, Z. W.; Wen, X.; Goodpaster, J. D.; Tonks, I. A. Mechanism of Ti-Catalyzed Oxidative Nitrene Transfer in [2 + 2 + 1] Pyrrole Synthesis from Alkynes and Azobenzene. *J. Am. Chem. Soc.* **2018**, *140* (23), 7267–7281.

(6) Baxter, R. D.; Sale, D.; Engle, K. M.; Yu, J.-Q.; Blackmond, D. G. Mechanistic Rationalization of Unusual Kinetics in Pd-Catalyzed C–H Olefination. *J. Am. Chem. Soc.* **2012**, *134* (10), 4600–4606.

(7) Nielsen, C. D.-T.; Burés, J. Visual Kinetic Analysis. *Chem. Sci.* **2019**, *10* (2), 348–353.

(8) Connelly, N. G.; Geiger, W. E. Chemical Redox Agents for Organometallic Chemistry. *Chem. Rev.* **1996**, *96* (2), 877–910.

(9) Evans, R.; Deng, Z.; Rogerson, A. K.; McLachlan, A. S.; Richards, J. J.; Nilsson, M.; Morris, G. A. Quantitative Interpretation of Diffusion-Ordered NMR Spectra: Can We Rationalize Small Molecule Diffusion Coefficients? *Angew. Chemie* **2013**, *125* (11), 3281–3284.

(10) Evans, R.; Dal Poggetto, G.; Nilsson, M.; Morris, G. A. Improving the Interpretation of Small Molecule Diffusion Coefficients. *Anal. Chem.* **2018**, *90* (6), 3987–3994.